Université de Lomé

Universität Rostock

DRP-CCDRM

INTERNATIONAL MASTER PROGRAMME IN ENERGY AND GREEN HYDROGEN

SPECIALITY: Bioenergy, Biofuels and Green Hydrogen Technology

MASTER THESIS

Subject/Topic:

SIMULATION OF BIOHYDROGEN PRODUCTION BY SEQUENTIAL DARK-PHOTO FERMENTATION OF PINEAPPLE WASTE

2023-2025

Presented on the 29th 09 2025

by:

Komlan Djiwonou WOENAGNON

Exam Committee members:

Chair:	Tizane DAHO, Professor, Université Joseph KI-ZERBO, Burkina Faso
Examiner/judge:	Kosi Mawuéna NOVIDZRO, Associate Professor, Université de Lomé -Togo
Main Supervisor :	Kokou N'WUITCHA, Professor, Université de Lomé - Togo
Co-Supervisor:	Satyanarayana NARRA, Professor, University of Rostock - Germany

WASCAL West African Science Service Centre on Climate Change and Adapted Land Use

Federal Ministry of Research, Technology and Space

Dedication

First, I dedicate this work to the almighty God for the good health, the wisdom, the strength and the peace of mind he granted me along this journey.

I would like also to dedicate this work to the loving memory of my father Kossi. Also, I would like to extend my deepest gratitude and dedicate this work to my sweet mother Enyonam, my sweetheart Catherine, my beloved son Wisdom and my wonderful siblings Eddy, Carine and Grégoire.

Acknowledgements

First, I would like to express my deep and sincere gratitude to the Federal Ministry of Research, Technology and Space (BMFTR) and the West African Science Service Center for Climate Change and Adapted Land Use (WASCAL) for providing me the necessary financial support to achieve this academic journey. I feel honored and grateful to receive this scholarship.

I extend my sincere gratitude to Prof. Adamou Rabani, rector of the University Abdou Moumouni (UAM) for his hospitality during the first and second semesters of this master's program.

I would also like to thank Prof. Adama M. Kpodar, the President of the University of Lomé for his warm welcome during the third semester specialization in bioenergy.

I also express my sincere gratitude to Prof. Dr. Elizabeth Prommer, Rector of the University of Rostock, as well as to Dr. Jan Tamm and Prof. Dr. Wolfgang D. Schareck, Chancellor and Vice Chancellor, respectively, for the internship opportunity at the Faculty for Agriculture, Civil and Environmental Engineering.

I express my heartfelt thanks to Prof. Komi Agboka, the director of the WASCAL GSP program at the University of Lomé, and the deputy Director Dr. Komi Begedou for their guidance and support at every step and stage of this master's program.

Additionally, I would like to thank Doctor Damgou MANI KONGNINE, the coordinator of Lomé's bioenergy, biofuels, and green hydrogen technology track for his unwavering support from the beginning of the programme. Without his unconditional support, I would not be participating in this programme. Thanks also to Dr. Mouhamed Idrissou, the scientific coordinator, for his excellent program management that made the outcome possible.

I especially thank my main supervisor Prof. Kokou N'wuictcha for his constant support, patience and encouragement since my bachelor's degree at the physics department at the University of Lomé. He spared no effort in supporting me throughout my training, spending sleepless nights with me in the laboratory to teach me the fundamentals of modelling and simulation. I will be forever grateful to him.

I express my gratitude to Prof. Dr. habil. Satyanarayana Narra, my co-supervisor and the General Coordinator of this Master's Speciality at Universität Rostock in Germany, for providing his valuable scientific and critical thinking inputs.

I am also very grateful to Prof. Tizane DAHO, the chair of the jury, and to Doctor Kosi Mawuéna NOVIDZRO, the examiner of the Jury, who despite their busy schedule, took time to thoroughly review the work and make constructive remarks to further improve it.

Special thanks to Mr. Djangbadjoa Gbiete, my daily supervisor, during my internship at the University of Rostock for his availability and precious advice since the early beginning of this journey.

Most importantly, I would like to thank all the staff members of the different WASCAL GSP programs at the University Abdou Moumouni and the University of Lomé, all the lecturers involved in the capacity building and the staff members for our internship at the University of Rostock.

I would like to thank the laboratory technicians, Mr. Kodjo and Mrs. Elvire, who have provided valuable time and assistance for experimental work.

Abstract

Biomass from agro-industrial waste represents a sustainable resource for bioenergy production. JUS DELICE, a pineapple processing factory in Togo generates large streams of waste but relies solely on composting as waste valorization pathway. As a result, the energy potential of the generated waste is still unexplored. On the other hand, Aspen Plus is a software widely used for the simulation of thermochemical processes. However, the software rooted in thermochemical processes is very limited in the simulation of biochemical processes due to the lack of built-in models for microbial kinetics, metabolic conversions, and inhibition effects.

This study investigated biohydrogen production using pineapple peels collected from JUS DELICE through three valorization pathways: dark fermentation, photo fermentation and the integrated sequential process. The peels were characterized through ultimate analysis, proximate analysis and fiber content and the data from characterization was used in Aspen Plus to simulate biohydrogen production under mesophilic conditions. The results revealed a good potential of pineapple peels for biohydrogen production with very high volatile solid content of 94.99% and high carbohydrates content on dry matter basis. It was also found that the integrated sequential process significantly improved the conversion process with a cumulative biohydrogen yield of 798.7 ml/gVS and a heating value conversion efficiency of 54.36%.

Key words: Pineapple peels, Aspen Plus, sequential dark-photo fermentation, biohydrogen.

Résumé

La biomasse provenant des déchets agro-industriels représente une ressource durable pour la production de la bioénergie. JUS DELICE, une usine de transformation d'ananas au Togo, génère de grands flux de déchets mais se base uniquement sur le compostage comme voie de valorisation des déchets. En conséquence, le potentiel énergétique des déchets générés reste encore inexploré. D'autre part, Aspen Plus est un logiciel largement utilisé pour la simulation des processus thermochimiques. Cependant, le logiciel ancré dans les processus thermochimiques est très limité dans la simulation des processus biochimiques en raison de l'absence de modèles intégrés pour la cinétique microbienne, les conversions métaboliques et les effets d'inhibition.

Cette étude a examiné la production de biohydrogène en utilisant des épluchures d'ananas collectées auprès de JUS DELICE à travers trois voies de valorisation : la fermentation sombre, la photo fermentation et la combinaison séquentiel intégré de ces deux processus. Les épluchures ont été caractérisées par une analyse élémentaire, une analyse proximale et la teneur en fibres, et les données de caractérisation ont été utilisées dans Aspen Plus pour simuler la production de biohydrogène dans des conditions mésophiles. Les résultats ont révélé un bon potentiel des épluchures d'ananas pour la production de biohydrogène avec une très haute teneur en solides volatils de 94,99 % et une haute teneur en hydrates de carbone sur base de matière sèche. Il a également été constaté que le processus séquentiel intégré améliorait significativement le processus de conversion avec un rendement cumulatif de biohydrogène de 798,7 ml/g VS et une efficacité de conversion du pouvoir calorifique de 54.36 %.

Mots-clés : Épluchures d'ananas, Aspen Plus, fermentation séquentielle sombre-photo, biohydrogène.

Acronyms and abbreviations

ADM 1: Anaerobic Digestion Model 1

ADF: Acid Detergent Fiber

ADL: Acid Detergent Lignin

AfDB: African Development Bank

CFE : Centre de Formalité des Entreprises

COD: Chemical Oxygen Demand

CSTR: Continuous Stirred Tank Reactor

DGE: Direction General de l'Energie

DIN: Deutsches Institut für Normung

ECREEE: Ecowas Center for Renewable Energy and Energy Efficiency

EU: European Union

GIZ: German Agency for International Cooperation

HDI: Human Development Index

HTR: Hydraulic Retention Time

IEA : International Energy Agency

INSEED : Institut National de la Statistique et des Etudes Economiques et Démographiques

IPCC: Intergovernmental Panel on Climate Change

ISO - International Organization for Standardization

IRENA: International Renewable Energy Agency

LPG : Liquefied Petroleum Gaz

LT2B : Laboratoire des Technologies de la Biomasse et de la Bioénergie

MC: Moisture Content

NDC: National Determined Contributions

NDL: Neutral detergent fiber

OLR: Organic Loading Rate

PROCAT : Projet d'appui à l'amélioration de la Compétitivité de la filière Ananas au Togo

SDG: Sustainable Development Goal

SIE: System d'Information Energetique

TS: Total Solid

VS: Volatile Solid

WASCAL: West African Science Service Center on Climate Change and Adapted Land Use

WHO: World Health Organization

List of tables

List of figures

Table of contents

Introduction

1.1 Background

Global climate change raises several concerns on energy systems in every jurisdiction given the huge contribution of energy production systems to greenhouse gas emissions. In recent days, more than 70 % of the global energy supply worldwide comes from exhaustible fossil fuels sources (IEA, 2022). This excessive use of fossil fuels paves the way for environmental problems such as global warming and air pollution, which cause health problems and affect the quality of life of populations. At present humans are already witnessing the adverse effects of climate change that encompasses rising temperatures, sea-level rise, drought, flooding, and more. About this worrying situation, the Intergovernmental Panel on Climate Change (IPCC) put emphasis on the need of global decarbonization now to mitigate climate change and ensure sustainable development (IPCC, 2022).

Energy is a backbone of complete production activity. It is involved in all sectors of activity and almost all production activity cannot operate without energy as it is a key aspect of a development process. A study conducted on the correlation between the Human Development Index (HDI) and energy consumption per capita revealed that countries with access to affordable energy are wealthier and more developed (Marcondes dos Santos & Perrella Balestieri, 2018). In this way, the Sustainable Development Goal 7 (SDG 7) aims to ensure access to affordable, reliable, sustainable and modern energy for all people worldwide. Yet, almost one half of the world's population still lack access to sustainable and reliable energy services (Ayaburi et al., 2020). The situation is worst in sub-Saharan African where, in 2021, more than 567 million people, accounting for more than 80% of the population did not have access to electricity. Furthermore, more than 906 million people in sub-Saharan Africa still lack access to clean cooking fuels and technologies and WHO estimates that 3.2 million premature deaths each year are linked to household air pollution caused by the use of polluting fuels (IRENA & AfDB, 2022; WHO, 2023).

Togo like any Sub-Saharan African country does not escape the scarcity of energy services, particularly in remote areas of the country. A recent study reveals that approximately 90 % of households in rural Togo are living under the threshold of energy poverty (Gafa et al., 2022). An assessment of the energy mix exhibits a large predominance of traditional biomass that accounts for 69% of the total energy supply. Petroleum products and electricity constitute 25% and 6% of the energy mix, respectively. The global access to electricity in 2021 is 63.7% but with large disparities between urban (85.2% access rate) and rural (25.0% access rate) areas. The electricity supply is covered by 42 % national production and 58% importation, highlighting a high external dependence contributing to high energy costs and energy insecurity. Petroleum products are entirely imported, and the biomass supply is 100% covered by national biomass supply (SIE, 2022). This excessive use of biomass coupled with a growing population that is forecasted to

double in the next three decades puts more pressure on natural biomass resources like forests of the country. The recorded deforestation rate is 422.15 km^2 per year, which corresponds to a contraction in forest cover of 0.74% per year between 1985 and 2020 (INSEED, 2022; Kombate et al., 2022).

Aware of the challenges of climate change and the decisive role of energy in the country's development, the Government in its 2030 roadmap has made the Sustainable Development Goals 7 and 13 priorities in the implementation of economic and social development initiatives. In the updated Nationally Determined Contributions (NDCs) of the country, the government aims to reduce its economy-wide emissions by 20.51%, to increase the share of renewable energies in the country's energy mix, to fight against deforestation and achieve 100% universal electrification by 2030 (NDC Partnership, 2021). Furthermore, bioenergy is identified as a key player in the country's renewable energy goals. In the recently published National Action Plan for Bioenergy, the government commits to reduce by 50 % the balance of firewood in the share of cooking energy by promoting Liquified Petroleum Gas (LPG), biogas and other forms of bioenergy. As far as the development of biofuels for transport is concerned, the targets set by the country aim to achieve a rate of 7% bioethanol in petrol consumption by 2030 and a rate of 10% biodiesel in diesel consumption by 2030 (ECREEE & DGE, 2024). The valorization of biomass waste for biohydrogen production aligns with the country's commitment to sustainable energy.

The pineapple sector in Togo is growing at a fast rate with the support of the PROCAT project in 2018, funded by the European Union (EU) and the German Agency for International Cooperation (GIZ) that intend to boost the sector's competitiveness. With such initiative, the pineapple production recorded significant improvements with a 50 % increase between 2019 and 2022. In fact, during this period, the national production has risen from approximately 30,000 tons to 44,000 tons and according to recent statistics, the sector generates on average more than 6 billion CFA francs per year (Ministère de l'agriculture, 2020; TOGO FIRST, 2022) . Regarding the added value of the sector to the country's economy, the government, in 2023, implemented a national investment action plan with the target to double the pineapple production by 2028 and increase the processing rate capacity from 35 % to 75 % with this time frame. The country counts in 2022 around fifty micro and small pineapple processors and registers also around twenty medium and large-scale processing units that transform pineapple into three main value chains: pineapple juice, dried pineapple and pineapple cocktail (Ministère de l'agriculture, 2023).

JUS DELICE SA, officially inaugurated on 25 April 2019 is an organic fruit processing factory with a social capital of 1 000 000 euro (CFE, 2018) in the district of Gbatopé in Tsévié, a headquarters of pineapple production in Togo. The industry received support from the Moringa fund and develoPPP a German corporation program. The factory occupies an area of 6,300 m^2 and

maintains high standards of food processing with physicochemical and bacteriological laboratories. More than 1,000 small producers around the industry, trained with standard rules of organic farming, provide the raw material used, which is pineapple. The factory uses smooth cayenne and sugar loaf varieties to satisfy its biological need for pineapple. The company has an automated production line with a processing capacity of 1.5 tons of fruit per hour generating 1,000 liters of juice per hour. The factory processes more than 25 tons of pineapple and generates more than 8 tons of waste daily. The company relies on composting platforms and ponds for waste management. Pineapple peels and pomace are used for composting to generate organic fertilizers that are given back to pineapple producers for soil amendment in pineapple growing. The large quantity of waste generated daily exhibits good potential for integrated pineapple biorefinery applications including bioenergy production from pineapple waste.

Aspen Plus is a powerful simulation tool used to explore process feasibility with the integration of different unit operations, estimation of energy and mass balance and techno-economic analysis (Yaashikaa et al., 2022). Yet, the software rooted in thermochemical engineering is not basically developed for biochemical processes like dark fermentation and photo fermentation. Only a few studies have been conducted on the simulation of biochemical processes using Aspen Plus simulation tool. Rajendran et al. (2014) developed a process simulation model of anaerobic digestion using Aspen Plus. The model used custom Fortran subroutines to incorporate the specific microbial growth rate and to access the impact of important parameters like ammonia inhibition, the effect of pH and volatile fatty acids inhibition. The model shows good agreement with real world data on laboratory and industrial scales and have been widely used as benchmark model in several studies to simulate anaerobic digestion using Aspen Plus. Nosrati-Ghods et al. (2020) implemented bioethanol fermentation simulation model that embeds a custom kinetic model into Aspen Plus. Factors such as ethanol inhibition, substrate inhibition, substrate limitation and biomass growth were developed using Aspen Custom Modeler and integrated into Aspen Plus to capture the complex biological behaviors of the process. The findings showed that the Aspen Custom Modeler integrated kinetics accurately predicted the fermentation process with less than 1% difference from industrial data. In contrast, the stoichiometric model showed about 9% difference from industrial data.

1.2 Problem statement

Solid waste management is of high importance in modern fruit processing industries like JUS DELICE for environmental protection and sustainability. As aforementioned, JUS DELICE relies solely on composting for solid waste valorization. While it is an eco-friendly solid waste management strategy that returns nutrients to the soil, it fails to explore the energy potential of the

total waste stream and its potential benefits. To date, no energy valorization pathways of the waste generated by JUS DELICE have been investigated.

As far as the simulation of biochemical processes such dark fermentation and photo fermentation is concerned, most studies reported in literature combine experimental work with kinetic modeling and simulation using tools like Python or MATLAB (Carreón et al., 2022; B. Kim et al., 2022; Lim & Nandong, 2022). Currently, only one work has been reported on the sequential integration of dark and photo fermentation using Aspen Plus simulation tool (Foglia et al., 2010). The mentioned work relied on equilibrium assumption and stoichiometry modeling based on the extent of reaction. Recently, Mokhtarani et al. (2025) investigated dark fermentation modeling and simulation in Aspen plus to explore technical bottlenecks of the process. Due to lack of data, the study was limited to a first-order approximation of power law kinetics to model the product formation and substrate degradation. The limitations of the current simulation assumption do not allow for accounting of inhibition effects (substrate inhibition, volatile fatty acids inhibition, ammonia inhibition, etc.), specific microbial growth rate, light dependency of photo fermentation, shifts in metabolic pathways, etc. These parameters are crucial to improve the accuracy of biochemical process simulation models. To date, there is a lack of Aspen Plus model which captures the full dynamic behavior of biochemical processes like dark fermentation and photo fermentation, or the integrated sequential process. This gap prevents realistic representation of biochemical processes using Aspen Plus simulation tool. If addressed this could improve the accuracy of biochemical processes design using Aspen Plus simulation tool, which will facilitate the optimization and the scale up of such processes. This study, therefore, attempts to fill this gap by building a process simulation model that relies on custom Fortran subroutines to account for these parameters.

1.3 Research questions

1. What are the key physicochemical properties of pineapple residues?
2. How do these properties influence their suitability as a feedstock for biohydrogen production through dark and photo fermentation?
3. What are the optimal conditions (pH, temperature, organic loading rate, light intensity, etc.) for hydrogen yield?

1.4 Research hypotheses

The hypotheses behind this research are formulated as follows:

1. The sequential combination of dark fermentation and photo fermentation allows us to achieve high biohydrogen yields compared to standalone processes.

2. The performance of biohydrogen production from pineapple peels is highly influenced by operating parameters such as the pH, the temperature, the organic loading rate and the hydraulic retention time.

1.5 Research objectives

This research aims to investigate biohydrogen production by sequential dark-photo fermentation of pineapple peels using Aspen Plus. The specific objectives are as follows:

1. To determine the physicochemical properties of pineapple residues used as feedstock.
2. To simulate the effects of the physicochemical properties of pineapple residues on the dark fermentation, photo fermentation and sequential dark-photo fermentation processes with Aspen Plus software.
3. To evaluate process parameters for sensitivity analysis and optimization.

1.6 Structure of the thesis

This thesis is divided into three main chapters in addition to an introduction and a conclusion.

1. **Introduction**: In this section the context and the motivations behind this study were presented. It also describes the goals of the study as well as the identified research questions.

2. **Chapter 1- Literature review:** This chapter covers published works in literature relevant to this topic. A review on hydrogen production by dark fermentation and photo fermentation as well as existing mathematical models for biohydrogen production are presented. In addition, the chapter highlights previous works on simulation of biochemical processes using Aspen Plus.

3. **Chapter 2- Material and Methods**: This chapter presents the material used to conduct this study as well as the various methods used to complete the research. It provides details on the experimental setup for pineapple peels characterization. In addition, a detailed account for the development of the simulation model and the validation of the simulation model using Aspen Plus has been explained.

4. **Chapter 3- Results and discussion**: In this chapter findings from the characterization of pineapple peels and simulation results are presented. A comprehensive analysis of the results from this study and their interpretation in relation to existing literature are presented.

5. **Conclusion**: This section summarizes the results from the current study, presents challenges and limitations of this work and provides recommendations and perspectives for future investigations on this topic.

CHAPTER 1: LITERATURE REVIEW

This chapter provides a literature review of biohydrogen production through biochemical conversion processes. It gives discussions about the underlying mechanisms behind processes like dark fermentation and photo fermentation and presents the advantages and drawbacks of each process. It also talks about the existing literature review of the different simulation models. It ends up with a brief overview on the implementation of anaerobic digestion as a biochemical process using Aspen Plus.

1.1 Pineapples processing waste

Pineapple industry from post-harvest to industrial processing generates huge amounts of waste. The main waste stream includes peel, core, crown and leaves which accounts between 50 and 60% of the total pineapple weight (Banerjee et al., 2018). The fruit processing into pineapple juice generates a wide variety of byproducts which can be valorized in a biorefinery framework as depicted in Figure 1.

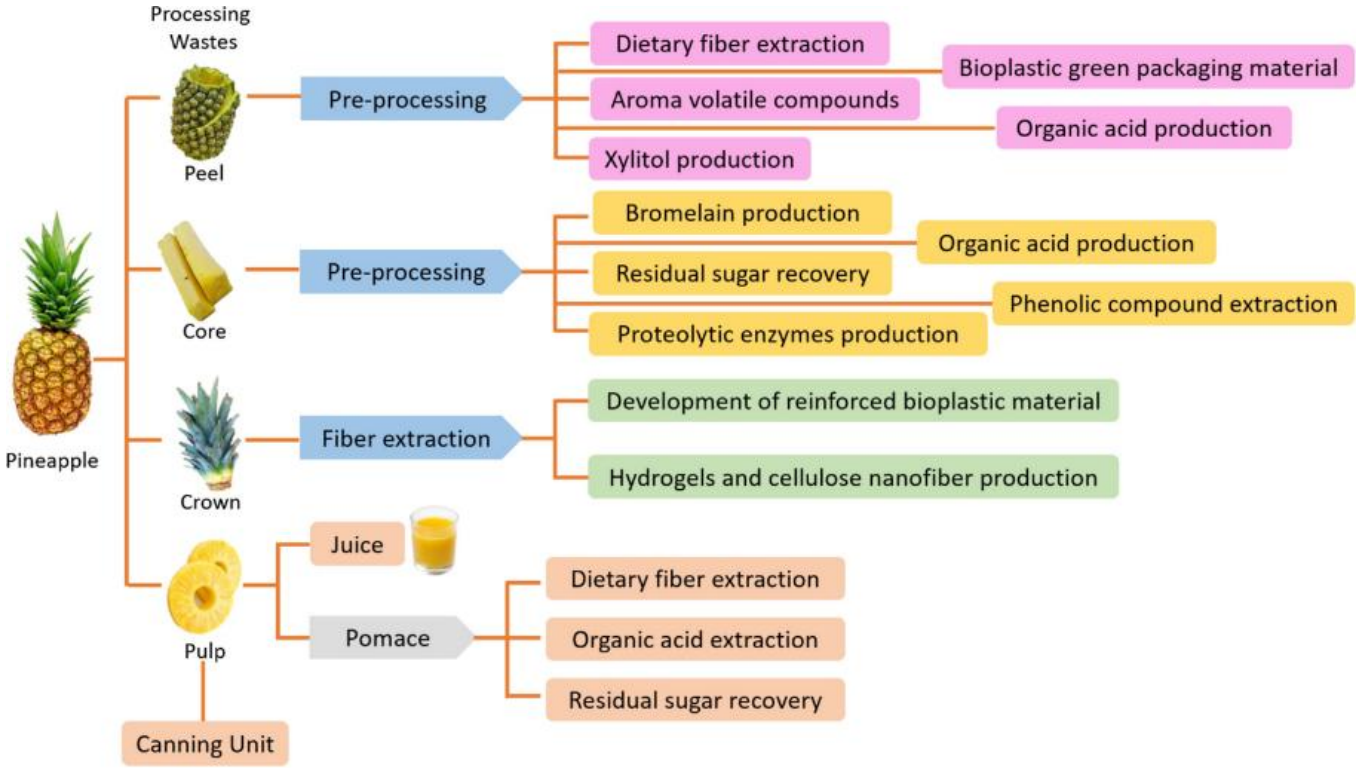

Figure 1: Biorefinery approach for pineapple waste utilization (Meena et al., 2022)

Depending on their chemical composition, these byproducts can be valorized through different value-added chemicals such as bromelain, xylitol, organic acids, dietary fiber or energy valorization pathways including bioethanol, biomethane and biohydrogen (Banerjee et al., 2018; Tiegam Tagne, Costa, Gupte, et al., 2024). Existing research on pineapple waste valorization revealed that it possesses intrinsic properties that make them a good candidate for bioenergy

conversion. The total carbohydrate content reported in the literature is in the range of 6.65 - 74.08 % for pineapple peels, and 7.21 - 83 % for pineapple core with important quantities of simple hydrolysable sugars such as glucose, fructose and sucrose (Paz-Arteaga et al., 2024). These unique properties make pineapple processing waste very attractive for energy valorization (Casabar et al., 2019; A. Chen et al., 2020; Mechery et al., 2024; Namsree et al., 2012).

1.2 Hydrogen production by dark fermentation

Dark fermentation is the most advanced and the most advantageous technology among biological hydrogen production routes. It is an environmentally friendly process used to produce biohydrogen and generate as the main byproduct, volatile fatty acids (acetic acid, lactic acid, propionic acid and butyric acid) and ethanol. Low cost and low energy demand, the process occurs in anaerobic conditions in total absence on light and uses a wide variety of organic compounds and wastewater rich in carbohydrates as substrates to produce hydrogen at a high rate (Hallenbeck & Ghosh, 2009).

The process, illustrated in Figure 2, is quite similar to the traditional anaerobic digestion process, well known for biogas production, a mixture of carbon dioxide and methane, a useful energy carrier.

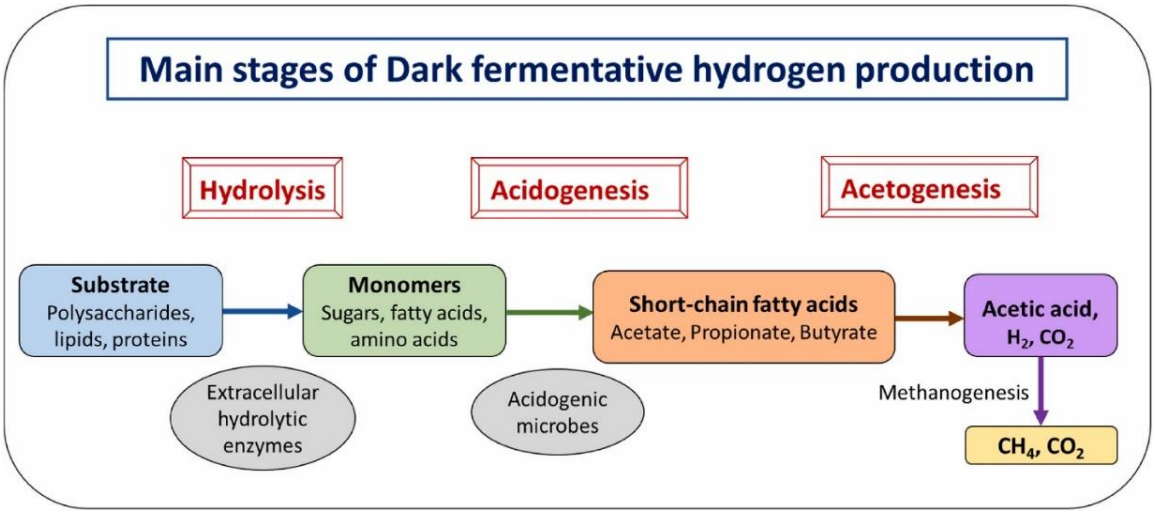

Figure 2: Main stages of Dark fermentative hydrogen generation (Palanivel et al., 2025)

Anaerobic digestion degrades organic matters in four stages namely hydrolysis, acidogenesis, acetogenesis and methanogenesis. Each step involves specific microorganisms to decompose the substrate through biological interactions. Hydrogen is mainly produced during the acidogenesis and acetogenesis steps as an intermediate metabolite but is used as electron provider by methanogens at the methanogenesis step to produce methane and CO_2. In addition to hydrogen production, the acidogenesis and acetogenesis steps result also in volatile fatty acids as the main byproduct. Then, it is possible to harvest hydrogen at the end of the acetogenesis step and left the

remaining volatile fatty acids for the methanogenesis step. Therefore, it is conceivable to bring some modification to the traditional anaerobic digestion process to prioritize hydrogen production. To do so, it is important inhibit methanogenic microorganisms and other hydrogen consuming bacteria and left in the medium only bacteria involved in the acetogenesis and methanogenesis stages (Lay, 2001; Logan et al., 2002; Sparling et al., 1997; C. C. Wang et al., 2003). Furthermore, it is crucial to control the operating parameters in favor of hydrogen production conditions. It includes maintaining the medium at a low pH, and reducing the hydraulic retention time to avoid the growth of methanogens (J. O. Kim et al., 2005; Mizuno et al., 2000).

1.3 Feedstock degradation pathways

The metabolic pathways of hydrogen production though dark fermentation process is depicted on Figure 3. It involves a wide group of facultative/obligate anaerobic bacteria performing a series of biological transformations on organic substrates to produce hydrogen, CO_2, volatile fatty acids (acetic acid, propionic acid, butyric acid) and alcohols. Dashed arrows on the Figure 3 indicate a process with multiple enzymatic steps (Ding et al., 2016).

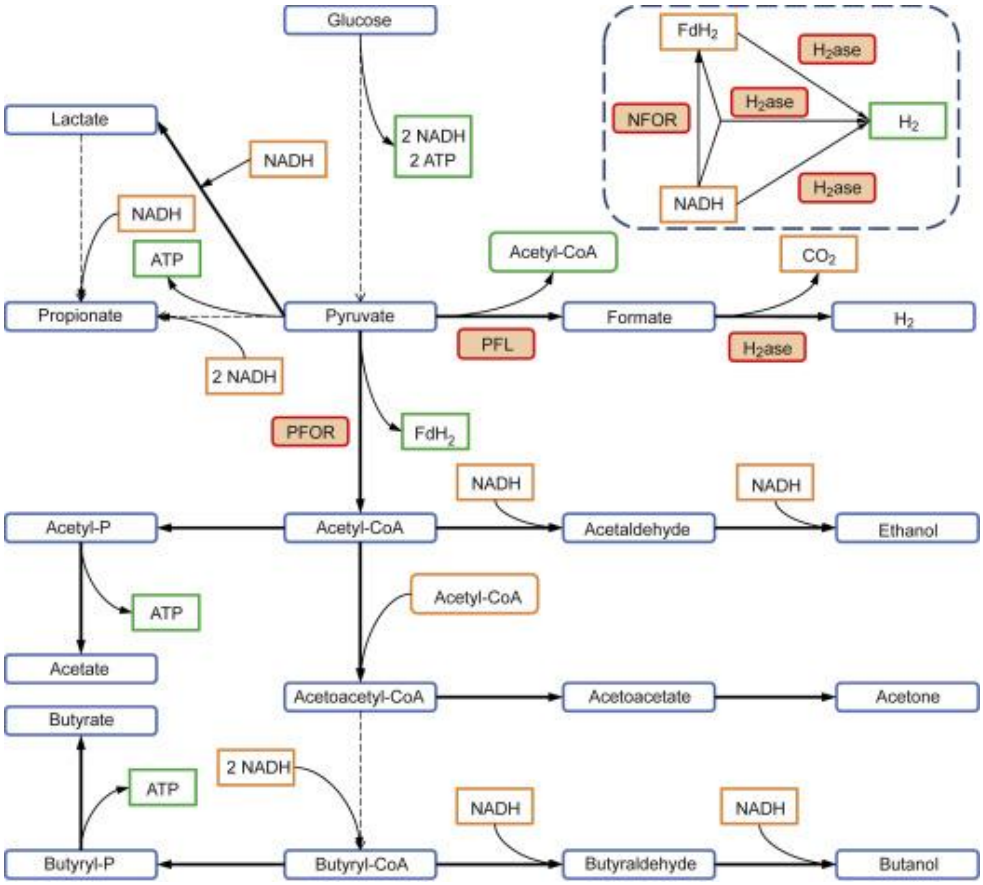

Figure 3: Hydrogen production pathway from glucose by fermentative microbes under anaerobic conditions (Ding et al., 2016)

Electron transfer in the process comes from two different stages of fermentation: the first is the substrate oxidation to pyruvate and the second is the conversion of pyruvate into volatile fatty acids and alcohols (Kraemer & Bagley, 2007). As far as the first stage is concerned, the oxidation of the substrate to pyruvate generates NADH, which is used by microorganisms like Firmicutes that possess the NADH (ferredoxin oxidoreductase: NFOR) to produce reduced ferredoxin. In the case of the second stage, depending on hydrogenases (hydrogen production bacteria) present on the site of the reaction, pyruvate can be converted either into acetyl-CoA and formate by pyruvate formate lyase (PFL) or acetyl-CoA and reduced ferredoxin by pyruvate-ferredoxin oxidoreductase (PFOR). Following the PFL pathway, some microorganisms make use of the formate hydrogen lyse complex that holds Ech hydrogenase, a special enzyme, to reduce protons (hydrogen formate lyase) into molecular hydrogen and produce CO_2 as byproducts (McDowall et al., 2014; Vardar-Schara et al., 2008). On the other hand, reduced ferredoxin is generated in the PFOR pathway. The reduced ferredoxin of this current stage and in the first stage by NFOR are oxidized by *Clostridium pasteurianum*, another type of hydrogenase to produce hydrogen. Furthermore, there are two other types of hydrogenases, one that can produce hydrogen directly from NADH (Hallenbeck, 2013), and the second one that can use NADH and reduced ferredoxin simultaneously to produce hydrogen (Schuchmann & Müller, 2012).

Following these pathways, both 5 carbon and 6 carbon sugars produce pyruvate as intermediate products during dark fermentation process. However, the most common mechanism described in literature is glycolysis. Then taking glucose as an example, from one molecule of glucose two molecules of pyruvate are generated through glycolysis. The generated pyruvate then continues the degradation process and enters the acidogenic pathways that are part of the hydrogen production process. In ideal conditions, up to 12 moles of hydrogen can be produced from 1 mole of glucose (Osman et al., 2023) through the dark fermentation process following by the equation (1) below:

$$C_6H_{12}O_6 + 6\,H_2O \longrightarrow 6\,CO_2 + 12\,H_2 \quad (1)$$

In practice, this performance is not achievable due to the complexity of the degradation pathways. The hydrogen yield per mole of glucose consumed is limited by metabolic constraints of dark fermentative hydrogen producing microorganisms due to the formation of byproducts such as acetic acid, acetone, etc. According to the theoretical limit, also known as “Thauer limit”, only a maximum of 4 mol of hydrogen, which represents 33% of the ideal hydrogen yield can be produced from 1 mole of glucose consumed when acetone or acetic acid is produced as a byproduct (Thauer et al., 1977). The biohydrogen yield following the different pathways of the dark fermentation process is expressed in equations (2) - (6) (Ding et al., 2016).

Acetic acid pathway:

$$C_6H_{12}O_6 + 2\,H_2O \longrightarrow 2\,CH_3COOH + 2\,CO_2 + 4\,H_2 \quad (2)$$

Propionic acid pathway:

$$C_6H_{12}O_6 + 2\,H_2 \longrightarrow 2\,CH_3CH_2COOH + 2\,H_2O \quad (3)$$

Butyric acid pathway:

$$C_6H_{12}O_6 \longrightarrow CH_3CH_2CH_2COOH + 2\,CO_2 + 2\,H_2 \quad (4)$$

Ethanol pathway:

$$C_6H_{12}O_6 \longrightarrow 2\,CH_3CH_2OH + 2\,CO_2 \quad (5)$$

Acetone pathway:

$$C_6H_{12}O_6 + H_2O \longrightarrow CH_3COCH_3 + 3\,CO_2 + 4\,H_2 \quad (6)$$

Apart from the Thauer limit, environmental conditions such as pH, temperature, microbial community hydrogen partial pressure, nutrients availability and substrate concentration also impact the efficiency of dark-fermentative hydrogen production. In addition , operating parameters like hydraulic retention time (HTR) and organic loading rate (OLR) cannot be overlooked (Gbiete et al., 2024; Ghimire et al., 2015).

1.4 Dark fermentation models for biohydrogen production

A model is a representation of real-life situations by means of mathematical equations. It plays a vital role in science, helping scientists to have a deeper understanding of complex systems and to develop strategies to forecast such systems. Systems involving biochemical processes are generally highly complex, with internal interaction and intricate biological pathways that may need to be considered. Nevertheless, several mathematical models for biohydrogen production have been developed. The existing models in the literature can be classified into two categories: microscopic models and macroscopic models. Macroscopic models rely on partial differential equations and the kinetics of chemical reactions to predict microbial growth, substrate consumption and production formation, whereas microscopic models use metabolic models on genomic scale to predict the evolution of the system (Gu et al., 2019; W. Wang et al., 2023). This section presents an overview of kinetic models of hydrogen production systems by dark fermentation. These models encompass the kinetic of microbial growth (biomass formation), the kinetic of products formation (hydrogen, volatile fatty acids, etc.), the impact of operating parameters (temperature, pH, hydraulic retention time, etc.) on product formation, the impact of

inhibitors and the relationship between substrate degradation rate, microbial growth rate and product formation rate (Boshagh et al., 2022; Nath et al., 2023; J. Wang & Wan, 2009b).

1.4.1 Kinetic models describing microbial growth rate and substrate consumption

Various bacteria species such as *Enterobacter*, *Clostridium*, Bacillus, etc. have been used to perform dark fermentation. As depicted in Figure 4 the growth phases of microorganisms in batch and fed-batch cultivations are lag phase, exponential phase, stationary phase, and death phase. The impact of the substrate concentration on a specific microbial growth rate can be described by the Monod model (Monod, 1949) expressed by equation (7):

$$\mu = \frac{\mu_{max} S}{K_s + S} \tag{7}$$

With: μ, the specific growth rate; μ_{max}, the maximum specific growth rate, K_s, the saturation constant; and S, the limiting substrate concentration. This model has been widely used to predict the evolution of hydrogen producing bacteria, especially at low substrate concentrations (W. H. Chen et al., 2006; Lee et al., 2008; Lo et al., 2008; Mu, Wang, et al., 2006). However, it has been reported that the model does not consider important parameters like inhibition caused by high substrate concentrations and pH (J. Wang & Wan, 2009b). Therefore, several modifications have been proposed to optimize the classical Monod model.

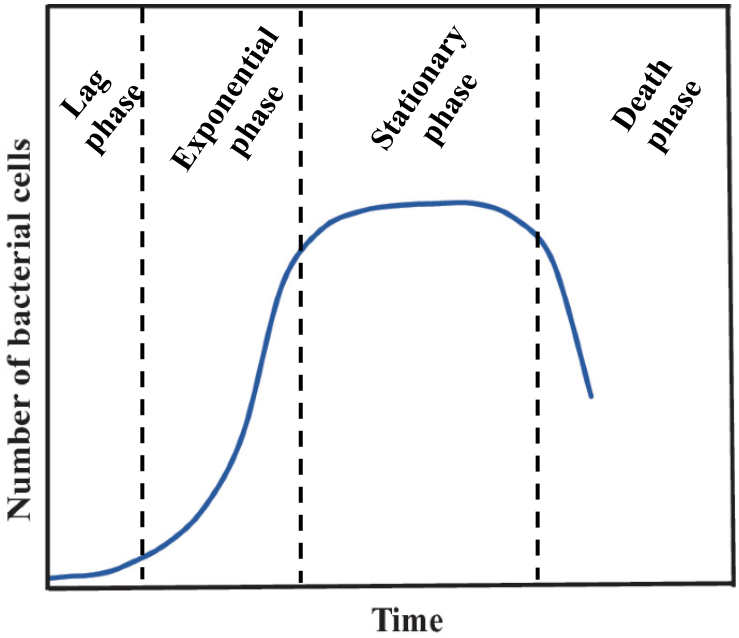

Figure 4: Curve of bacterial growth phases of microbial culture in batch systems (Khasa & Mohanty, 2021)

1.4.2 Kinetic models describing inhibition effects

To consider the substrate inhibition effect, several studies introduce an inhibition factor in the classical Monod. The Andrews' model (Equation (8) (Andrews, 1968) is popular and widely used among these improvements of the Monod model.

$$\mu = \frac{\mu_{max} S}{K_s + S + \frac{S^2}{K_i}} \tag{8}$$

K_i is the inhibition constant.

The Andrews' model, despite its ability to predict the inhibition impact of the substrate, does not give information on the nature of the inhibition. Han and Levenspiel (1988) proposed a generalized form of the Monod model (Equation (9) which forecast both substrate stimulation at low concentration and substrate inhibition at high concentration.

$$\mu = \mu_{max} \frac{S\left(1 - \frac{S}{S_{max}}\right)^n}{S + K_s\left(1 - \frac{S}{S_{max}}\right)^m} \tag{9}$$

Where S_{max} is the maximum substrate concentration, n and m are constant parameters indicating the type of substrate inhibition (competitive, uncompetitive, non-competitive and mixed inhibition).

1.4.3 Kinetic models describing product formation

The end products of the dark fermentation process include products in gaseous phase (hydrogen, CO_2 and methane) and products in liquid phase (volatile fatty acids and solvents). The modified Gompertz equation (10) is widely used to estimate the cumulative hydrogen production during the dark fermentation in batch process (Zwietering et al., 1990).

$$H(t) = H_{max} \exp\left\{-exp\left[\frac{R_{max} e}{H_{max}}(\lambda - t) + 1\right]\right\} \tag{10}$$

With: H(t), the cumulative hydrogen production; H_{max}, the maximum gas production potential; R_{max} , the maximum gas production rate; λ the lag time and t , the cultivation time.

Mu, Zheng, et al. (2006) expressed the modified Gompertz equation in more general form to forecast not only the cumulative hydrogen production, but also to predict the formation of volatile fatty acids.

1.5 Hydrogen production by photo fermentation

1.5.1 Overview of the process

Like dark fermentation, photo fermentation is a biochemical process for hydrogen production. The process relies on photosynthetic bacteria like purple non sulfur bacteria to convert organic substrates (sugar, volatile fatty acids, lignocellulosic biomass, etc.) into biohydrogen in the presence of light (Hallenbeck, 2009; Melitos et al., 2021). The process is operated in photobioreactors and is mainly influenced by the medium parameters (temperature, pH, light intensity, carbon and nitrogen sources, presence of metal ions, etc.), the photobioreactor configuration (flat panel, tubular, etc.), and the microbial community (Tiang et al., 2020). Purple non sulfur bacteria is the main microbial community involved in photo fermentative biohydrogen production due to their metabolic flexibility and versatility in substrate consumption. Most commonly used strains include *Rhodobacter sphaeroides*, *Rhodobacter capsulatus*, *Rhodopseudomonas* species such as *Rhodopseudomonas palustris*, *Rhodopseudomonas capsulate* etc. (Gupta et al., 2024). As aforementioned, these photosynthetic bacteria are versatile and can convert a wide variety of waste substrates. However, the low light conversion efficiency (less than 10 %), a low hydrogen production rate, the high design and operation cost of photobioreactors are important setbacks for large scale implementation of photo fermentation (Akbari & Mahmoodzadeh Vaziri, 2017; Zainal et al., 2024).

1.5.2 Metabolic pathways

The different steps followed by photo fermentative strains in hydrogen production are shown in Figure 5. The underlying mechanism of the process lies in electron transfer through light absorption without oxygen generation using hydrogen as an electron donor for halogenated organic compounds hosted by several microbes (Gupta et al., 2024). The process starts with absorption of light energy by photosynthetic bacteria. The bacteria use light energy to create a proton gradient which serves to generate ATP. This ATP helps electron transfer through the cell's metabolism. The key enzyme behind the process is nitrogenase which uses electrons and ATP to reduce protons, generating hydrogen. Under normal conditions, nitrogenase functions as a catalyst in the reduction of nitrogen (N_2) to ammonia with release of hydrogen (Equation (11). However, in the absence of nitrogen, nitrogenase keeps working and produces hydrogen from protons (Equation (12) (Sağır et al., 2018).

$$N_2 + 8H^+ + 8\,e^- + 16\,ATP \rightarrow 2\,NH_3 + H_2 + 16\,ADP + 16\,Pi \quad (11)$$

$$2H^+ + 2e^- + 4\,ATP \rightarrow H_2 + 4\,ADP + 4\,Pi \quad (12)$$

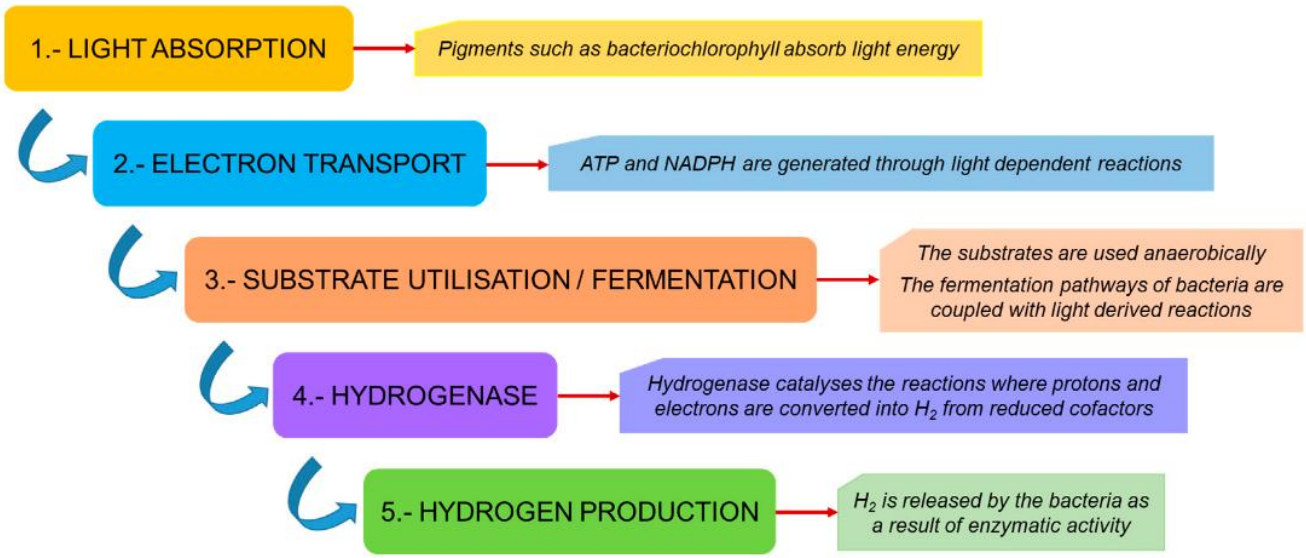

Figure 5: A general outline of hydrogen production by photo-fermentative bacteria (Gupta et al., 2024)

1.6 Mathematical models for photo fermentation

Literature reported various kinetic models used to predict the progress of photo-fermentative hydrogen production systems. Similar to dark fermentation, most of these models rely on classical models such as Monod model and its modifications, Gompertz model, etc. (Akbari & Mahmoodzadeh Vaziri, 2017; Gadhamshetty et al., 2008). Evidently, these models are limited in the description of process key variables. Therefore, different modifications include additional terms to study particular effects. Modified versions of the original Monod models have been used to describe the impact of light intensity on the cell growth (Tamiya et al., 1953; Zhang et al., 1998). The impact of light exposure on the microbial growth of photosynthetic bacteria can be investigated using Equation (13) below (Gadhamshetty et al., 2008):

$$\mu = \frac{\mu_m C_S}{K_S + C_S + \frac{C_S^2}{K_{Xi}}}\left(1 - \frac{C_X}{C_{Xm}}\right)\left(\frac{I}{K_{XI} + I + K_I I^2}\right) \quad (13)$$

With: μ, the growth rate; μ_m, the specific growth rate; C_S, the substrate concentration; C_X, the substrate inhibition constant; C_{Xm}, the maximum value of the cell concentration at which level growth will cease; K_S, the half saturation constant; K_I, the inhibition constant; K_{XI}, the light saturation constant; I, the light intensity.

The second order light intensity term accounts for the negative impact of the light intensity on the cell growth. The smaller is the value of K_I, the greater is the impact of light inhibition on cell growth (Sasikala et al., 1991).

The kinetic of product formation, considering the influence of light intensity, substrate inhibition can be described using Equation (14) adapted from the Luedeking–Piret equation (Gadhamshetty et al., 2008; X. W. Zhang et al., 1998).

$$\frac{dC_P}{dt} = \left(Y_{PX}\frac{dC_x}{dt} + \mu_{PX}C_x\right)\frac{C_s}{K_{PS} + C_S + \frac{C_S^2}{K_{Pi}}}\left(\frac{I}{K_{PI} + I + K_{PI}I^2}\right)\left(1 - \frac{C_P}{C_{Pm}}\right) \quad (14)$$

With: C_P, product concentration; Y_{PX}, the yield coefficient of the product; μ_{PX}, non-growth associated to product formation rate; C_x, the cell concentration; C_S, substrate concentration; K_{PS}, the half saturation constant for substrate; K_{Pi}, substrate inhibitory constant; K_{PI}, light saturation constant; I, light intensity; C_{Pm}, maximum product concentration.

1.7 Overview of sequential dark-photo fermentation

In the dark fermentation process, the overall hydrogen yield is relatively low due to accumulation of volatile fatty acids. However, the process is still attractive because it produces hydrogen at high levels and the reactor is simple to design (Ahmad et al., 2024; Dzulkarnain et al., 2022). Therefore, to maximize the hydrogen yield and achieve high substrate conversion efficiency, dark fermentation can be combined with second stage systems such as photo fermentation, microbial electrolysis cell, anaerobic digestion, etc. As far as the combination, dark plus photo fermentation is concerned, it can be done either sequentially or be integrated in a single reactor, also known as dark-photo co-fermentation (Zhang et al., 2020). However, the sequential process is preferred to the one-stage co-fermentation as it facilitates the application of optimum conditions to bacterial populations in both reactors. In co-fermentation both bacterial communities have different optimum conditions which are difficult to satisfy together (Zagrodnik & Duber, 2024). Despite all these advantages, the sequential process also presents some drawbacks. Majority of photosynthetic bacteria perform under neutral pH. On the other hand, effluent from dark fermentation is usually rich in volatile fatty acids. Therefore, dilution of the effluent is required, which brings additional costs. In addition, the effluent is rich in fix nitrogen, which inhibits nitrogenase, the key functional enzyme of photosynthetic bacteria. The high cost of the photoreactor is also an important setback (Hallenbeck, 2013). Reported hydrogen yields of the sequential process are in the range of 5-7 mol H_2 per mol of glucose (Hallenbeck, 2013; Sağır et al., 2018).

1.8 Anaerobic digestion process simulation using Aspen Plus

In the literature, research has been done on the simulation of anaerobic digestion using different existing simulations software that include SuperPro Designer, Biowin, Simba, MATLAB/ Simulink and Aspen Plus. Aspen Plus offer rigorous property methods and meticulous thermodynamic calculations.

Rajendran et al. (2014) designed a process simulation model of anaerobic digestion using Aspen Plus to predict the biogas production from any feedstock at any given process condition. The process simulation model involves the intermediary metabolisms of all four phases of anaerobic fermentation by using a set of 46 chemical reactions and it also includes inhibitions, rate-kinetics, pH, ammonia, volume, loading rate, and retention time. The Non-Random Two-Liquid (NRTL) model property method, and a stoichiometric and continuous stirred tank reactor were used for hydrolysis and the remaining phases of the anaerobic digestion process, respectively. The developed model was validated against 7 different cases which include laboratory, as well as industrial data. A p-value of 0.701 was found after statistical analysis of the results from the simulation model and real results, which mean that there is no significant difference between the two results.

Al-Rubaye et al. (2019) developed a simulation model of anaerobic digestion process using Aspen Plus to forecast biogas production from wastewater, cattle and cow manure. The model relied on the non-random two liquid model (NTRL) for the calculation of activity coefficients and mole fractions. Furthermore, the simulation model uses a stoichiometric reactor for the hydrolysis and a continuous stirred tank reactor for acidogenesis, acetogenesis and methanogenesis steps. The simulation was run in thermophilic conditions (55-60° C). For the purpose, the feedstock is heated before its introduction in the stoichiometric reactor for hydrolysis. The process simulation model was validated against experimental results for cattle manure, cow manure and distillery wastewater. The results showed that an increase in the feeding rate decreased methane composition in the biogas due to low residence time on the biomass in the reactor. Furthermore, a sensitivity analysis of hydrogen injection on the yield of biogas revealed that an optimum introduction of hydrogen in the process increases the methane composition in the biogas by 40%.

An anaerobic digestion process simulation model was implemented by Ravendran et al. (2019) using Aspen Plus. The study used cow dung as substrate and focused on how the substrate flow rates and operating pressure impact the biomethane yield. The impact of hydrogen injection was also investigated. Three stoichiometric reactors are used to implement the different stages of the anaerobic digestion process, one for hydrolysis, one for acidogenesis and acetogenesis and one for methanogenesis. The model also includes one mixer and two heaters for mixing the substrate stream and maintaining the process under mesophilic conditions. Furthermore, a flash drum was included to purify the producer gas. The model was validated against real data. The results showed that feed flow rate of 0.36 L/day, at hydrogen flow rate of 180 L/day, and at pressure of 3 bars resulted in the optimal yield of bio-methane of 0.122 kg/day with a purity of 74.2% in biogas production.

Aguilar et al. (2017) designed a process simulation model following the research conducted by Rajendran et al. (2014). After validation, the model was used to simulate biogas production under thermophilic and mesophilic conditions. The anaerobic co-digestion of food waste and primary sludge under different mixing ratios of 1:2, 1:1, and 2:1 was simulated for hydraulic retention time of 21 days and for three different organic loading rates: 2.08, 2.49 and 3.34 gvs l^{-1} day $^{-1}$. Furthermore, the anaerobic digestion model was coupled with a combined heat and power system also developed using Aspen Plus. The obtained results indicated that biogas production is optimal for a mixing ratio of 1:2 at a mass flow of 132.42 tons/day under both thermophilic and mesophilic conditions.

Lorenzo-Llanes et al. (2020) implemented a simulation model in Aspen Plus for UASB reactor for anaerobic digestion of vinasses. The simulation flow sheet comprises two stoichiometric reactors (one for hydrolysis and one for methanogenesis) and two continuous stirred tank reactors (one for acidogenesis and one for acetogenesis) in addition to one mixing unit before the hydrolysis and separation units after the methanogenesis step. The developed model includes anaerobic digestion model 1 (ADM 1) flow pattern, biofilm characteristics and sulfate reduction process. It was validated against laboratory results as well as data from pilot and industrial scales with a mean relative error lower than ±15%. In agreement with the experimental results, the model successfully predicts the failure of the reactor at a laboratory scale for SO_4^{2-}/COD ratio between 0.01 and 0.1 and higher than 0.1 respectively and a decrease of 5% in biomethane yield. Furthermore, a sensitivity analysis conducted on the granule size revealed that the biogas production rose by 16% when the granule diameter dropped from 4 mm to 1 mm.

CHAPTER 2: MATERIALS AND METHODS

This chapter presents the materials and the methodology used to perform this study. It starts with the description of the feedstock used in this study, the different characterizations operated on the feedstock and describes the model design using Aspen Plus to simulate dark fermentation, photo fermentation and sequential dark-photo fermentation processes. In Addition, the process configuration followed by the choice of the different reactors and the selection of system process parameters are described.

2.1 Sample collection and preparation

The feedstock used in this research is a fresh mixture of pineapple peels and pomace from the pineapple juice production process as illustrated in Figure 6. The sample was collected directly from JUS DELICE in an airtight bag to reduce its microbial activity and transported immediately to the Laboratory of Biomass and Bioenergy Technologies at the University of Lomé (LT2B: Laboratoire des Technologies de la Biomasse et de la Bioénergie). Upon arrival, subsamples were prepared for the proximate analysis, and the remaining sample was oven dried at 105 °C for 24 hours, ground and stored in an airtight bag for subsequent analysis at the University of Rostock.

Figure 6: Pineapple waste from juice production process

Figure 7 shows the schematic diagram of the technology used to conduct this research. As depicted on the diagram, the process starts with the characterization of pineapple peels through proximate analysis, ultimate analysis and fiber content. The data obtained from the feedstock characterization was used as input data to simulate biohydrogen production through standalone dark fermentation, standalone photo fermentation and sequential dark-photo fermentation using Aspen Plus software.

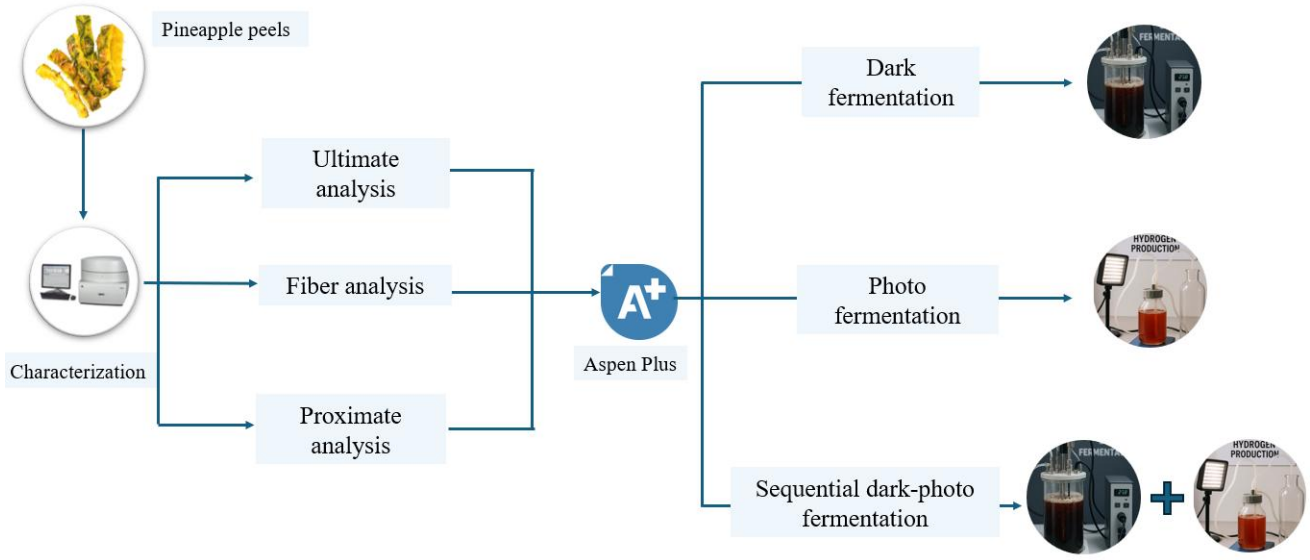

Figure 7:Schematic diagram of the research methodology

2.2 Feedstock characterization

2.2.1 Proximate analysis

The Thermogravimetric analyzer, LECO TGA 701 is used for the proximate analysis of the biomass. The biomass was grinded to obtain sample size less than 1 mm. Approximately 2 g of samples (triplicate) were used for the analysis. For the moisture content, the samples were heated from room temperature to 105° C in an inert atmosphere (nitrogen). Afterward the samples were heated to 800° C for volatile matter determination. Finally, the samples were burned in pure oxygen around 815° C to determine the ash content. The moisture content (MC), the total solid (TS), the volatile matter content (VM) and the ash content are calculated using the following formulae (equations (15) - (18)).

$$MC = 100 \times \frac{m_1 - m_2}{m_1} \quad (15)$$

$$TS = 100 \times \frac{m_2}{m_1} \quad (16)$$

$$VS = 100 \times \frac{m_2 - m_3}{m_1} \quad (17)$$

$$Ash = 100 \times \frac{m_4}{m_1} \quad (18)$$

With, m_1: the mass of the fresh sample, m_2: the mass of the sample after heating to 105 ° C, m_3: the mass of the sample after heating to 800 ° C and m_4: the mass of the residue after burning the sample in oxygen.

2.2.2 Ultimate analysis and heating values

The feedstock was crushed and the powder obtained was homogenized before the ultimate analysis. The nominal top sample size was 1 mm or less following the recommendations of DIN EN ISO 21646 (2022-09) standards. The elemental composition of the feedstock in terms of carbon (C), hydrogen (H), nitrogen (N), are determined according to DIN EN ISO 21663 (2021-03) standards. A complete combustion of the feedstock was performed at high temperature in pure oxygen and the combustion gases were analyzed. The oxygen content was determined based on the recommendations of DIN 51733 (2016-04) standards. The sulfur content was accessed using calorimetric digestion method following DIN EN 15408 (2011-05) recommendations. The aqua regia flux digestion method was used to determine the trace elements and heavy metal content of the feedstock based on the recommendations of DIN 22022-2 (2001-02) standards. The gross heating value and the net heating value were determined using bomb calorimeter, according to DIN EN ISO 21654 (2021-12) standards.

2.2.3 Fiber analysis

Neutral detergent fiber (NDL), acid detergent fiber (ADF) and acid detergent lignin (ADL) are used to assess the cellulose, hemicellulose and lignin content of the biomass sample. The analysis was conducted using Fibrebags dried at 105° C for 1 hour and afterwards the weight of the empty Fibrebags was recorded as m_1. To start, the samples were dried at 105° C for 24 hours and then the dried samples were ground to reduce the size of particles to less than 1 mm. For the ADF determination, 1 g of sample portion was weighed. The weight of the sample in the Fibrebags was recorded as m_2. Then a glass spacer was introduced in each Fibrebag and both were placed in the sample carousel. After this step, the Fibrebags were rinsed with hexane to remove the excess fat from the samples. Then, the samples were introduced in the Fibretherm for washing with ADL solution. After washing the samples were dried overnight at 105° C and the measured mass was recorded as m_4. After the previous step, for the ADL determination, the Fibrebags are hung in a

sample carousel and secure. The sample carousel with the Fibrebags was placed in a 5 L beaker and covered at room temperature with 72 % sulfuric acid. The sulfuric acid was maintained at a temperature of 20° C to 33° C for three hours and the mixture was stirred every hour. The Fibrebags are washed with hot water to the neutral point at the end of the previous step and dried at 105° C for 24 hours. The recorded mass for this step is m_7. After drying the Fibrebags were placed in a muffle furnace for at least two hours for ashing. Then a cooling down was operated in a desiccator and the measured mass was m_5.

The process for NDF determination starts similar to the process of ADF determination. After the washing step with the hexane solution to remove excess fats, the Fibrebags are placed in the Fibretherm for further washing with NDF solution. Afterward the spacer is removed from each Fibrebag and one of the samples was carefully discharged. The Fibrebag was then placed in the crucible rolled up and dried at 105° C 24 hours. After cooling down the mass was determined (m_9) and then the ashing of the Fibrebag was operated at 500° C for 2 hours at least. A subsequent cooling down was operated and the mass (m_9) of the samples determined. The NDF, ADF, ADL as well as the cellulose, hemicellulose and lignin content are calculated using the following expressions (Equations (19)- (24))(Liebetrau et al., 2016).

$$ADF(\%TS) = \frac{(m_4 - m_1) - (m_5 - (m_6 - m_3)}{((m_2 - m_1) \times TS) \times 100} \times 100 \quad (19)$$

$$ADL(\%TS) = \frac{(m_7 - m_1) - (m_5 - (m_6 - m_3))}{((m_2 - m_1) \times TS) \times 100} \times 100 \quad (20)$$

$$NDF(\%TS) = \frac{(m_4 - m_1) - (m_5 - (m_6 - m_3))}{((m_2 - m_1) \times TS) \times 100} \times 100 \quad (21)$$

$$Lignin(\%TS) = \text{ADL} \quad (22)$$

$$Hemicellulose(\%TS) = \text{NDF - ADF} \quad (23)$$

$$Cellulose(\%TS) = NDF - (Hemicellulose + Lignin) \quad (24)$$

2.3 Process design in Aspen Plus

2.3.1 Biomass feedstock and simulation components definition

The simulation of the dark fermentation process using pineapple peels as feedstock starts with the definition of the different parameters involved in the process. From previous works existing in the literature, pineapple peels are rich in carbohydrates (cellulose and hemicellulose), and also contain lignin, proteins and lipids (Mala et al., 2024). This complex aspect of the feedstock made it difficult to be represented by a single chemical formula or a single component in Aspen Plus. Therefore,

the pineapples peels are user-defined in the current work as a non-conventional component "PEELS" using physicochemical properties of the feedstock obtained from proximate analysis and ultimate analysis. The component PEELS thus defined exhibits chemical properties that can be used to approximate the real feedstock in the process. The remaining components are retrieved from local Aspen Plus data banks. Carbohydrates and lignin are defined as biomass solid, intermediate fermentation products and final fermentation products are defined as conventional components. The property method used for the simulation is the NTRL (Non-Random Two Liquid) method for its ability to calculate activity coefficients of the component and to simulate vapor-liquid phases (Rajendran et al., 2014).

2.3.2 Dark fermentation process flow diagram

The simulation of the dark fermentation process was divided into three parts: the upstream, the reactor unit and the downstream.

The upstream process as illustrated on Figure 8 includes a size reduction unit, a mixing unit, a pump and a heater. The process started with the material stream PEELS modeled as a non-conventional solid stream (NC Solid) using data from the proximate analysis and the ultimate analysis of the feedstock on a dry basis. The simulation is designed to handle 1.5 tons of dried pineapple peels per day, and the feedstock was given a random particle distribution size between 20 and 200 mm. The PEEL material then enters the size reduction unit SHRED where it is reduced to a smaller particle size. After the size reduction, the feedstock fed to the RYIELD unit where the yield distribution of carbohydrates and lignin were allocated following the results of the fiber analysis. The yield distribution of cellulose, hemicellulose and lignin are reported in Table 1.

Afterward the feedstock was fed to the mixing unit where it was mixed with water to obtain the desired substrate concentration. The mixed stream was pumped and then passed through a heat exchanger where it was heated to weaken chemical bonds before entering the hydrolysis step.

Table 1: Yield distribution of cellulose, hemicellulose and lignin

Component	Distribution (%wt.)
Cellulose	15.82
Hemicellulose	27.79
Lignin	3.06

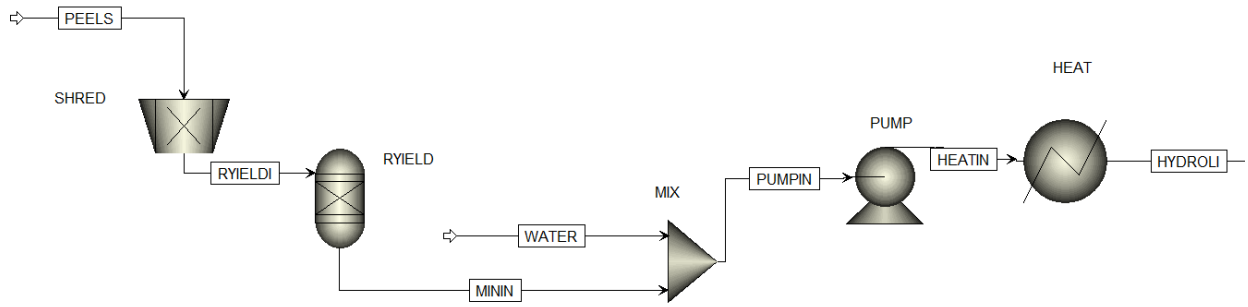

Figure 8: Upstream process

The dark fermentation process was simulated following the four steps of anaerobic digestion, namely hydrolysis, acidogenesis, acetogenesis, and methanogenesis. The simulation of the reactor relied on a previous process simulation model developed by Rajendran et al. (2014) on anaerobic digestion with some key assumptions. These assumptions include:

- Hydrogen inhibitors such as methanogens were inactive with the heat pretreatment of the slurry.
- Methanogenesis was considered negligible within the hydraulic retention time.
- Only cellulose and hemicellulose were considered as carbohydrate sources in this work.
- Proteins and fats were negligible due to their low concentration in pineapple peels.
- The process occurred under anaerobic conditions.
- The volume of the feedstock was assumed negligible compared to the volume of water in the simulation.

Hydrolysis, the first step of the process is a complex and a rate-limiting step in the overall process (Guo et al., 2021). Based on the initial composition and the bioavailability of the respective substrates, different fractions of sugars, amino acids, glycerin and long fatty acids are produced during hydrolysis (Ruzicka, 1996; Schattauer et al., 2011). In the current study, based on the previous assumptions, only hydrolysis of cellulose and hemicellulose were considered. A stoichiometric reactor, represented by the block HYDROLY in Figure 9 is used for the simulation based on the extent of the reaction as specified by (Rajendran et al., 2014). The monomers released from the hydrolysis step are fed to the Continuously Stirring Tank Reactor (CSTR) where the acidogenesis and acetogenesis steps take place. The occurring reactions for the acidogenesis and acetogenesis steps are simulated on a kinetic basis. It is worth noting that these sets of reactions follow a very complex metabolic pathway making it difficult to study the kinetics of such reactions. Due to this reason, only a few kinetic studies of specific microorganisms, usually using glucose as substrate have been reported (Mokhtarani et al., 2025). In the present study, for simplicity,

hydrogen yield from dark fermentation is modeled as first order kinetic following the Equation (25).

$$R_{H_2} = kS \tag{25}$$

With R_{H_2} the rate of hydrogen production, S the substrate concentration and k the rate constate given by the Arrhenius expression (Equation (26)):

$$k = k_0 \exp\left(\frac{-E}{RT}\right) \tag{26}$$

Where: k_0, is the pre-exponential factor; E, the activation energy; T, the temperature and R, the ideal gas constant (Mokhtarani et al., 2025).

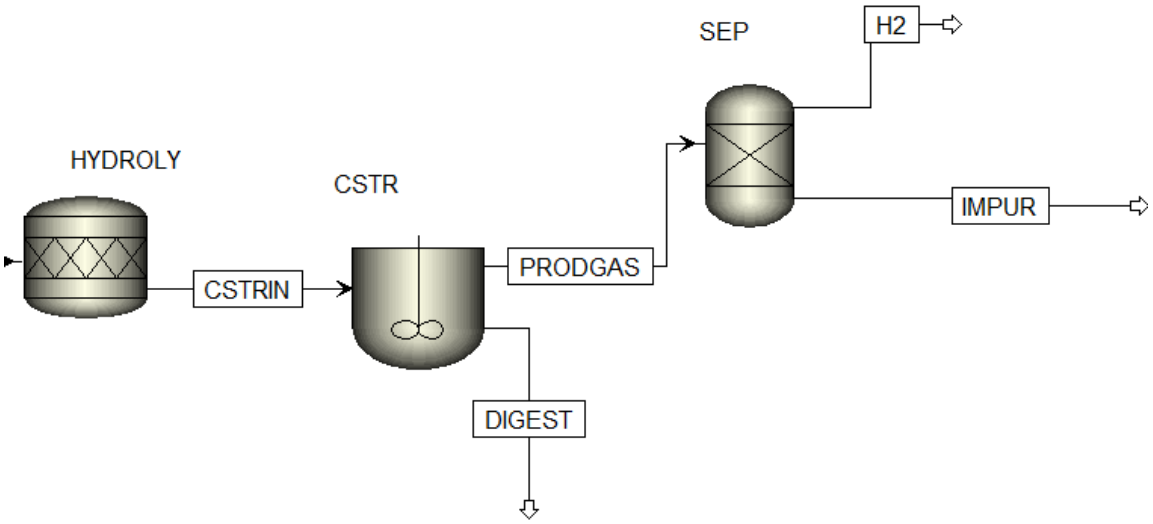

Figure 9: Dark fermentation reactor units and gas upgrading

The set of reactions for hydrolysis, acidogenesis and acetogenesis are summarized in Table 2. The kinetic constants for acidogenesis and acetogenesis and extent of hydrolysis reaction are retrieved from previous research in literature (Bechara, 2022; Khamtib & Reungsang, 2012; Rajendran et al., 2014). After the reactor units, the producer gas undergoes an upgrading process via the SEP unit (Figure 9) where hydrogen is separated from the other gases. The hydrogen cumulative yield is given by the Equation (27):

$$H_{2_{yield}} = \frac{V_{H2}}{m_{VS}} \tag{27}$$

Where: V_{H2} (L), is the volume of biohydrogen produced and m_{VS} (kg), the mass of volatile solids. $H_{2_{yield}}$, is the cumulative biohydrogen yield expressed in mL/g VS.

Table 2: Chemical reactions of dark fermentation steps(Bechara, 2022; Khamtib & Reungsang, 2012; Rajendran et al., 2014)

Step	Main Reactant	Stoichiometry	Extent of Reaction/ Kinetic constant
Hydrolysis	$CELLULOSE$	$(C_6H_{10}O_5)_n + nH_2O \rightarrow nC_6H_{12}O_6$	0.4 ± 0.1
	$HEMICELLULOSE$	$(C_5H_5O_4)_n + nH_2O \rightarrow \frac{5}{2}n\ CH_3COOH$	0.5 ± 0.2
	$HEMICELLULOSE$	$(C_5H_8O_4)_n + nH_2O \rightarrow nC_5H_{10}O_5$	0.6 ± 0.0
	$XYLOSE$	$C_5H_{10}O_5 \rightarrow C_5H_4O_2 + 3H_2O$	0.6 ± 0.0
	$CELLULOSE$	$(C_6H_{10}O_5)_n + nH_2O \rightarrow \rightarrow 2\ n\ CH_3CH_2OH + 2nCO_2$	0.4 ± 0.1
	$ETHANOL$	$2\ CH_3CH_2OH + CO_2 \rightarrow CH_4 + 2\ CH_3COOH$	0.6 ± 0.1
Acidogenesis	$GLUCOSE$	$C_6H_{12}O_6 \rightarrow \frac{3}{4}\ C_3H_6O_2 + \frac{1}{2}\ C_4H_8O_2 + \frac{7}{4}\ CO_2 + \frac{7}{4}\ H_2$	$9.54 * 10^{-3}$
	$XYLOSE$	$C_5H_{10}O_5 \rightarrow \frac{5}{3}\ H_2 + \frac{5}{6}\ C_4H_8O_2 + \frac{5}{3}\ CO_2$	$5.45 * 10^{-3}$
	$XYLOSE$	$C_5H_{10}O_5 + \frac{5}{3}\ H_2O \rightarrow \frac{5}{3}\ CO_2 + \frac{10}{3}\ H_2 + \frac{5}{3}\ CH_3COOH$	$3.46 * 10^{-3}$
Acetogenesis	$PROPIONIC\ ACID$	$CH_3CH_2COOH + H_2O \rightarrow \frac{3}{2}\ CH_3COOH + H_2$	$1.95 * 10^{-7}$
	$ISOBUTYRIC\ ACID$	$C_4H_8O_2 + 2H_2O \rightarrow 2\ CH_3COOH + 2\ H_2$	$5.88 * 10^{-6}$

The organic loading rate is given by Equation (28):

$$OLR = \frac{m_{feed} * VS}{V} \quad (28)$$

With: OLR, representing the organic loading rate; VS, the volatile solid content of the feedstock; m_{feed}, the mass of the feedstock on dry basis per day; and V, the working volume. The Table 3 shows information about the parameters used for the simulation of dark fermentation.

Table 3 : Simulation parameters for dark fermentation

Parameters	Values
OLR (g VS/L/day)	10
Temperature (° C)	40
Pressure (atm)	1
HRT (days)	10

The sensitivity to hydraulic retention time (HTR), and organic loading rate were investigated in the current study. The HTR was in a range of 1 to 10 days with regular increments of 0.5 day. The OLR varied from 5 to 30 g VS/L/day with regular increments of 5 g VS/L/day.

The heating value conversion efficiency was calculated using Equation (29).

$$HCE = \frac{m_{H_2} * HHV_{H_2}}{m_{peels} * HHV_{peels}} \quad (29)$$

With: *HCE*, the heating value conversion efficiency; m_{H_2}, the mass of biohydrogen produced from the process; HHV_{H_2}, the higher heating value of hydrogen; HHV_{peels}, the higher heating value of pineapple peels; m_{peels}, mass of pineapple peels used in the process.

2.3.3 Photo fermentation and sequential dark-photo fermentation

The process simulation flow sheet of the photo fermentation process was similar to the flow sheet developed for the dark fermentation process illustrated by Figure 8 and Figure 9. However, some operating conditions and the set chemical reactions occurring and the related kinetics were modified. The photoreactor is modeled by a CSTR unit. The hydrolysis step was the same as in dark fermentation (Table 2). The stoichiometric relationships of hydrogen production from xylose and glucose are expressed as follows as shown in Table 4:

Table 4:Stoichiometry of glucose and xylose conversion in photo fermentation (Pattanamanee et al., 2015)

Main reactant	Stoichiometry	Kinetic constant
Xylose	$C_5H_{10}O_5 + 5H_2O \rightarrow 10H_2 + 5CO_2$	$3.16 * 10^{-6}$
Glucose	$C_6H_{12}O_6 + 6H_20 \rightarrow 6CO_2 + 6H_2$	$1.62 * 10^{-6}$

The kinetic constants rates k for glucose and xylose conversion are derived from experimental data of consumption rates of xylose and glucose by Rhodobacter sphaeroides S10 retrieved from the literature (Pattanamanee et al., 2015). The value of the constant rate was derived by fitting the corresponding consumption rate to first order kinetic model. At the operating conditions, data available in the literature suggest optimal temperature range from 30° C - 35° C to support microbial activity for efficient hydrogen production in photo fermentation (Ji & Wang, 2021). Therefore, the fermentation was simulated as continuous isothermal process at 35 ° C and 1 atm, with initial substrate concentration of 10 gVS/L for 72 hours like in dark fermentation process. Aspen Plus does not have a built-in unit operations block to model the impact of light intensity on light-dependent processes. Therefore, the model did not include light conversion efficiency, and it was assumed that the fermentation process occurred under sufficient and optimal light intensity leading to the reactions in Table 4.

The sequential dark-photo fermentation process was modeled as a two-stage continuous process operating in series. The process flow sheet of the dark fermentation step was identical to the flow sheet presented in Figure 8 and Figure 9 with the same chemical reactions and operating

conditions. After the CSTR unit, the digestate from dark fermentation entered a separation unit where liquid and solid phases of the digestate were separated into two different streams. Afterwards, the liquid digestate was used as substrate to feed a second CSTR unit where volatile fatty acids from the dark fermentation process undergo further conversion into biohydrogen. The gaseous stream coming from the photo fermentation of volatile fatty acids was fed into the separation unit to separate hydrogen from other gases. The flow sheet of the sequential dark-photo fermentation process is shown in Figure 10. The underlaying chemical reaction of the transformation of volatile fatty acids are expressed by the equations shown in Table 5.

Table 5: Reactions involved in the conversion of volatile fatty acids (Uyar et al., 2009)

Main reactant	Stoichiometry	Kinetic constant
Acetic acid	$C_2H_4O_2 + 2H_2O \rightarrow 4H_2 + 2CO_2$	$6.67 * 10^{-6}$
Propionic acid	$C_3H_6O_2 + 4H_2O \rightarrow 7H_2 + 3CO_2$	$1.48 * 10^{-6}$
Butyric acid	$C_4H_8O_2 + 6\,H_2O \rightarrow 10H_2 + 4CO_2$	$4.17 * 10^{-6}$

The consumption rate constants were found to fit first order kinetics with high accuracy (R^2 in the range of 0.86 and 0.99). The consumption rate constant, using first order kinetics of acetic acid and butyric acid are 0.002 h^{-1} and 0.001h^{-1} respectively (Uyar et al., 2009). The kinetic constant of propionic acid consumption was determined from data provided by Ventura et al. (2016) on propionic acid consumption using first order kinetics.

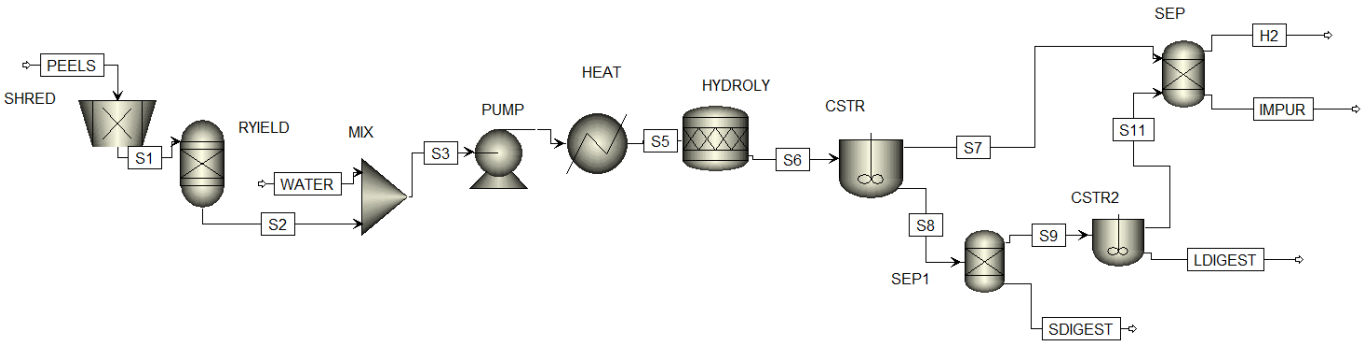

Figure 10:Sequential dark-photo fermentation flowsheet

2.4 Model validation

2.4.1 Dark fermentation

Validation of simulation models is a crucial step in any simulation work to ensure the reliability of the simulation results. It can be done by conducting laboratory experiments or using secondary data from laboratory results or real-world cases. In the current study the simulation was validated

using secondary data from previous laboratory experiments under similar conditions. It is important to note that this model does not consider microbial activity, hence only the kinetics of chemical reactions involved in the process were considered. For the validation, two cases were considered, based on laboratory investigations conducted by Tiegam Tagne et al. (2024). The first case is pineapple peels with a substrate concentration of 2 gVS/L and the second case is cassava peels with the same substrate concentration as pineapple peels. Both cases are conducted for hydraulic retention time of 6 days at 40° C and 1 atm. The simulation results are in good agreement with the experimental results, as depicted in *Figure 11*.

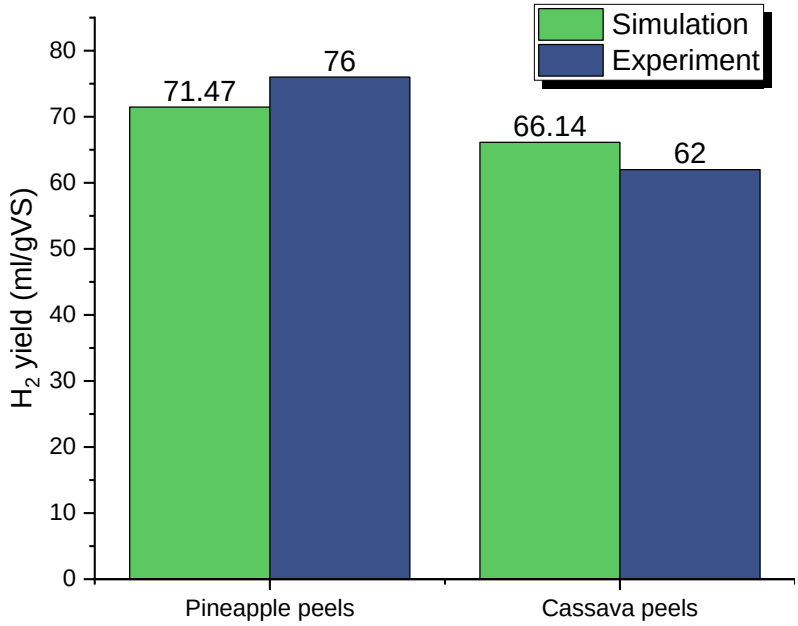

Figure 11: Quantitative validation of the dark fermentation simulation model

2.4.2 Photo fermentation

The main validation criteria used to validate the photo fermentation model is cumulative hydrogen production. Two cases were considered in this validation. For the first case, corn stalk hydrolysate have been used with a concentration of 5 g/L of corn stalk in a photo fermentation process with 6 days hydraulic retention time (Yang et al., 2015). The second case is obtained from Zhang et al. (2020) in which corn straw have been used as substrate with 12 days hydraulic retention time. For both cases, the difference between the simulated results and experimental results was less than 15 %. The bar chart of Figure 12 shows the comparison of simulated and experimental results for the two cases.

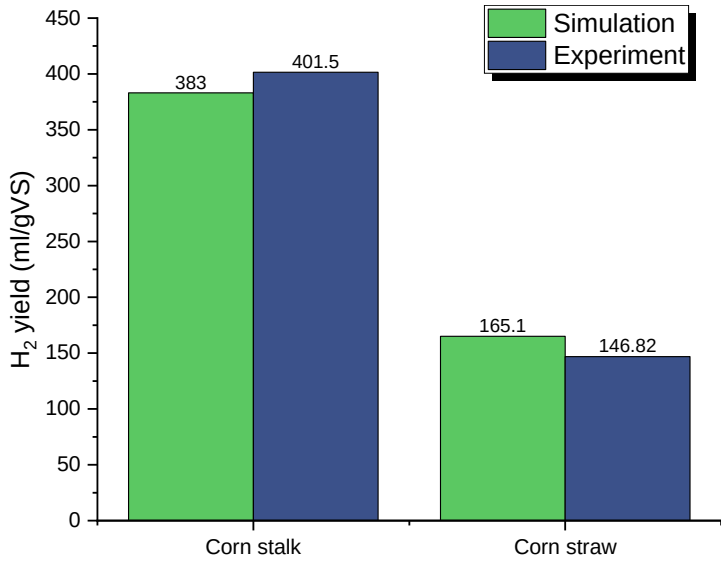

Figure 12:Quantitative validation of the photo fermentation simulation model

CHAPTER 3: RESULTS AND DISCUSSION

This chapter presents the findings from the pineapple peels characterization as well as the simulation results of the different hydrogen production pathways described in chapter 2. Pineapple peels properties are discussed in terms of their suitability for biochemical conversion processes. The simulation results are discussed in terms of hydrogen yield and heating value conversion efficiency. Furthermore, the gaps between the current results and relevant reported data in the literature are also analyzed.

3.1 Feedstock properties

3.1.1 Ultimate analysis and heating values

In the Table 6 are shown the elemental composition and the heating values of pineapple peels on a dry weight basis. Overall, carbon, oxygen and hydrogen represent the highest proportions with 44.6, 44.3 and 6.06%, respectively. Nutrient elements such as nitrogen and phosphorus are present in low proportions in the pineapple peels. The low content of nitrogen can be explained by the relatively low protein percentage of pineapple peels reported in the literature (Gharge et al., 2024; Tiegam Tagne et al., 2024). The C/N ratio and C/P of the feedstock are respectively 56.17 and 343.

On the other hand, the low sulfur content (0.1 %) of the biomass is beneficial for biochemical conversion. It is important to notify that sulfur content of biomass leads to the formation of hazardous products like hydrogen sulfide (H_2S) which not only is toxic to hydrogen production bacteria and corrosive to the equipment, but also requires extensive purification of the gas produced, which increases the production cost of biohydrogen. Dhar et al. (2012) conducted research on sulfur inhibition in dark fermentation and reported that a low concentration (25 mg/L) in sulfide allows to increase biohydrogen yield by 54%, whereas high sulfide concentration drastically decreases the biohydrogen production by 90%. Therefore, low sulfur content allows to minimize H_2S production and increase in the meantime the biohydrogen yield. Mineral elements like potassium (K), magnesium, sodium and calcium are also detected in very low amounts, less than 1% except potassium (1.03%). These elements, despite to have been present in very low amounts, are beneficial for biochemical processes as they support bacterial growth and microbial activity of hydrogen producing bacteria (Wang & Wan, 2009a; Yao et al., 2013). The gross heating value of 17.8 MJ/kg (Table 6) is in good agreement with the findings of Azevedo et al., (2021) who reported 17.7 % MJ/kg for the higher heating value of pineapple peels.

Table 6: Ultimate analysis and heating value of pineapple peels on dry weight basis

Ultimate analysis	
Element	**wt. %**
C	44.6
O	44.3
H	6.08
N	0.79
P	0.13
S	0.1
Fe	0.011
Mg	0.14
K	1.03
Ca	0.48
Na	0.13
Si	0.11
Heating values (kJ/kg)	
HHV	17827
LHV	16502

3.1.2 Proximate analysis and fiber analysis

The data presented on the pie chart of Figure 13 show the proximate composition of pineapple peels on a dry weight basis. As illustrated on the graph, the feedstock had 1% moisture content, and this extremely low value of the moisture content makes sense as the pineapple peels were oven dried for 24 hours to avoid feedstock degradation and to facilitate its transportation. When looking at the chart, the VS accounts for 95 % of the pineapple peels on a dry matter basis. In comparison, research by Paepatung & Nopharatana. (2009) on pineapple peels reported VS value of 93.6 % (wt. %) on a dry basis. As the volatile solid indicates the fraction of feedstock that can be converted through biochemical pathways, high volatile solid content is an indication of more organic material available for biochemical conversion (Parra et al., 2025). The ash content of 4 % is in good agreement with the ash content values (4.1%) in the literature (Azevedo et al., 2021; Dai et al., 2020; Madureira et al., 2018).

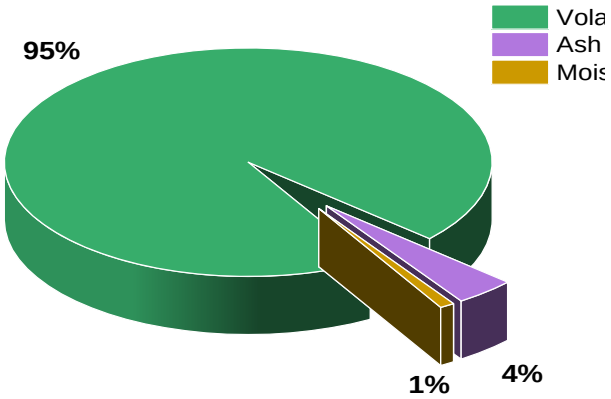

Figure 13: Proximate analysis on dry weight basis of dried pineapple peels (wt.%)

The bar chart of Figure 14 depicts the percentage of cellulose, hemicellulose and lignin of the pineapple peels on a dry weight basis. Overall, it can be seen that the feedstock has low lignin content, relatively high hemicellulose content and moderate cellulose content. The reported values for cellulose, hemicellulose and lignin content of the feedstock are found in the ranges reported in the literature (Azevedo et al., 2021; Banerjee et al., 2018, 2019; Tiegam Tagne et al., 2024). Hemicellulose and cellulose are the sources of C5 and C6 sugar platforms. Due to the crystalline structure of cellulose, it degrades slower than hemicellulose during hydrolysis step of the fermentation process. However, the high content of carbohydrates is a good indicator for biochemical conversion processes as good pretreatment of the feedstock may release high amounts of carbohydrate during hydrolysis. Another important aspect of the feedstock is the low lignin and ash content, which is favorable for biochemical conversion. In fact, with such low values, the risk of microbial inhibition is minimal, and the biodegradability of the feedstock is improved, subsequently improving the biohydrogen yield (Li et al., 2016).

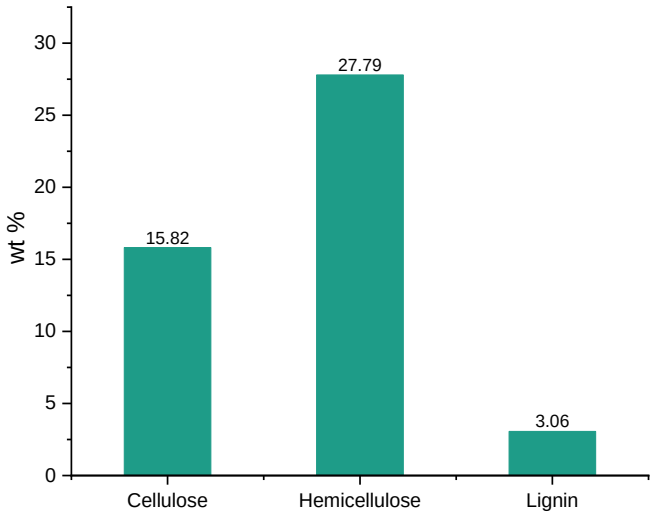

Figure 14: Fiber analysis on dry weight basis

3.2 Biohydrogen production

3.2.1 Biohydrogen yields in dark fermentation

Simulation of biohydrogen production through single stage dark fermentation using pineapple peels as main substrate was investigated. The profiles of biohydrogen yield performance and sugar concentrations in the bioreactor are recorded in Figure 15. It is clear from the graph that glucose and xylose concentration dip within the first hours of fermentation, while the cumulative hydrogen increases quickly in the first 24 hours. According to what is shown in the graph, glucose and xylose concentration sharply decreased from 8 and 4 mM/L respectively to near zero. Glucose is reported to be metabolized at a higher rate (Kádár et al., 2004), therefore the high consumption rate of glucose observed during the acidogenesis phase is justified. However, xylose is known to exhibit slower degradation rate in acidogenesis, and usually when mixed with glucose, xylose metabolism is delayed until glucose is exhausted (Ren et al., 2008). It is worth noting that the kinetic data used to describe xylose consumption rate in this model are derived from xylose conversion by *Thermoanaerobacterium thermosaccharolyticum*. This strain have been reported to consume simultaneously xylose and glucose at similar rates (Khamtib & Reungsang, 2012), explaining the high consumption rate of xylose depicted in Figure 15. Following the rapid consumption of simple sugars, a phase correlated with high biohydrogen production in the initial 24 hours, the hydrogen yield continues to increase despite the substrate depletion. This upward trend can be explained by the subsequent conversion of volatile fatty acids, which were accumulated during the acidogenesis phase, into hydrogen and carbon dioxide during acetogenesis. The hydrogen yield after 72 hours is greater than 80% of the overall hydrogen yield after 10 days of hydraulic retention time. In addition, from Figure 15, it clearly appears that after 96 hours of hydraulic, the biohydrogen yield exhibits an asymptotic trend. This suggests that the optimal hydraulic retention time is in the range of 3 to 4 days.

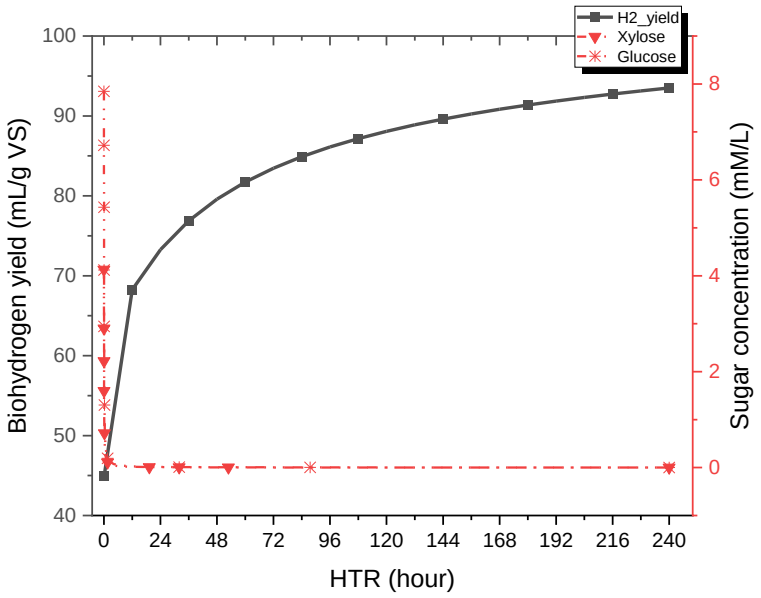

Figure 15:Cummulative hydrogen yield and sugar consumption in dark fermentation

The cumulative hydrogen yield starts at just around 45 mL/g VS within the first hours of fermentation. The cumulative hydrogen yield accelerates during the first five days of fermentation and hits 88 mL/gVS at the end of the fifth day. This fast accumulation of biohydrogen can be explained by the predominance of acidogenesis and acetogenesis at the beginning of the process which favor biohydrogen production. After the first five days of retention time, a steady increase in cumulative hydrogen yield is observed for the next five days. This can be explained by the depletion of carbon sources or the accumulation of volatile fatty acids within the first days of fermentation. Overall, 93.5 mL/g VS of hydrogen was produced after 10 days of hydraulic retention time. Compared to values reported in the literature on biohydrogen production using fruit waste as substrates (Table 7), this result is lower than the ones reported by Magama et al. (2021) and Kharisma et al. (2022).

Table 7: Biohydrogen yield from dark fermentation of fruit waste reported in literature

Type of substrate	H_2 production (mL/g VS)	Reference
Pineapple peels	76	(Tiegam Tagne et al., 2024)
Fruit and vegetable waste	52	(Cieciura-Włoch et al., 2020)
Pineapple peels	91.80	(Tiegam Tagne et al., 2024)
Fruit and vegetable waste	142.74	(Magama et al., 2021)
Melon fruit waste	228.2	(Kharisma et al., 2022)
Pineapple peels	93.5	This study

3.2.2 Influence of the organic loading rate

Biohydrogen yield at different organic loading rates (OLR) was investigated. The organic loading rate varied in the range of 5 g VS/L/day to 30 g VS/L/day with regular increment of 5 g VS/L/day. In the Table 8 are shown the simulated results of cumulative hydrogen yield after 10 days of hydraulic retention time. Overall, what stands out from the table is that there is an upward trend of cumulative hydrogen yield. The cumulative hydrogen yield starts at 84 mL/g VS (OLR = 5 g VS/L/day) and jumps to 96 mL/g VS at an organic loading rate of 15 g VS/L/day. Following this, the trend exhibits relatively stable cumulative hydrogen yield from an organic loading rate of 20 g VS/L/day and above. This trend suggests an optimal organic loading rate between 20 and 25 gVS/L/day. The graph shown in Figure 16 presents the time course of variations of cumulative hydrogen yield at the different organic loading rates discussed above. Overall, the trend of the data presented on the graph confirmed previous observations (Table 8). Several investigations were conducted on the impact of organic loading rate on biohydrogen yield in dark fermentation. From data available in the literature, there is no universal relationship between biohydrogen yield and organic loading. In fact, some systems may perform better at lower organic loading rate while others achieve good results at higher organic loading rates (Tawfik & Salem, 2012). However, different optimal values of organic loading rate are reported, depending on the type of substrate and operating conditions. Above the optimal value, several studies reported instability issues and decrease of biohydrogen production (Pérez-Rangel et al., 2023; Tawfik & Salem, 2012). The steady increase in cumulative hydrogen yield at high organic loading rate can be attributed to the important accumulation of volatile fatty acid and process instabilities at high organic loading rates. It is worth noting that the current model does not consider inhibitory effects such as ammonia inhibition, volatile fatty acids inhibition, increase of hydrogen partial pressure, etc. The introduction of these effects could potentially lead to a dip in biohydrogen production, especially at high organic loading rates.

Table 8: Impact of organic loading rate on cumulative hydrogen yield in dark fermentation

OLR (g VS/L/day)	**H_2 yield (mL/g VS)**
5	84.46
10	93.45
15	96.42
20	97.89
25	98.77
30	99.35

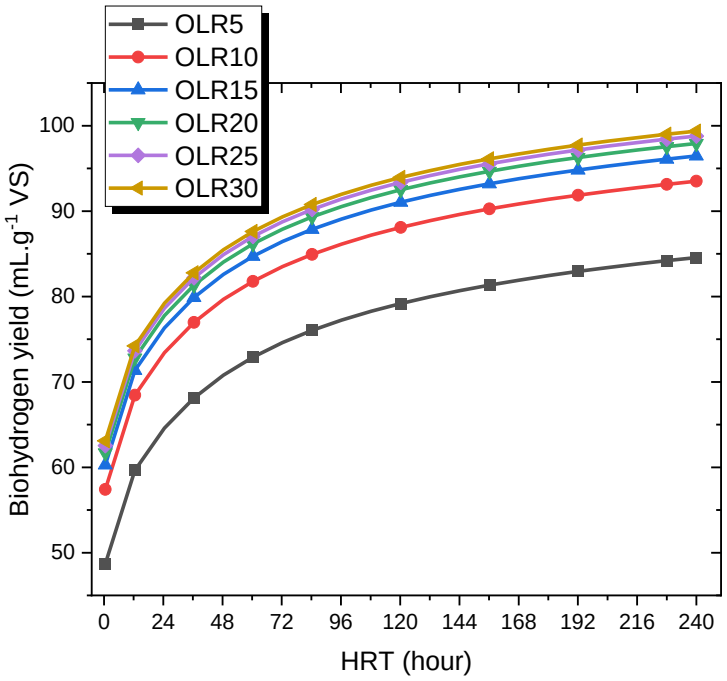

Figure 16:Biohydrogen yield at various organic loading rate

3.2.3 Accumulation of volatile fatty acids

The graph reported on Figure 17 gives information about the accumulation of volatile fatty acids in the bioreactor during the dark fermentation process. At the early stages of the process, the concentration of propionic acid and butyric acid sharply increased, peaking at around 7.8 mM/L and 7.6 mM/L respectively within the first six hours of fermentation. In the meantime, the concentration of acetic acid also increased exponentially reaching 82 mM/L. This step corresponds to the acidogenesis phase, for which in the present model acetate, propionate and butyrate pathways were all considered. Following this step, butyric acid concentration experienced a dramatic fall while propionic acid fell gradually. At the same time, acetic acid experienced modest increase in concentration. This step corresponds to the acetogenesis phase during which propionic and butyric acid undergo further transformation to hydrogen and acetic acid. After 10 days of hydraulic retention time, acetic acid concentration topped at 94 mM/L , propionic acid concentration slid to 6.7 mM/L and butyric acid concentration dropped to 1.3 mM/L.

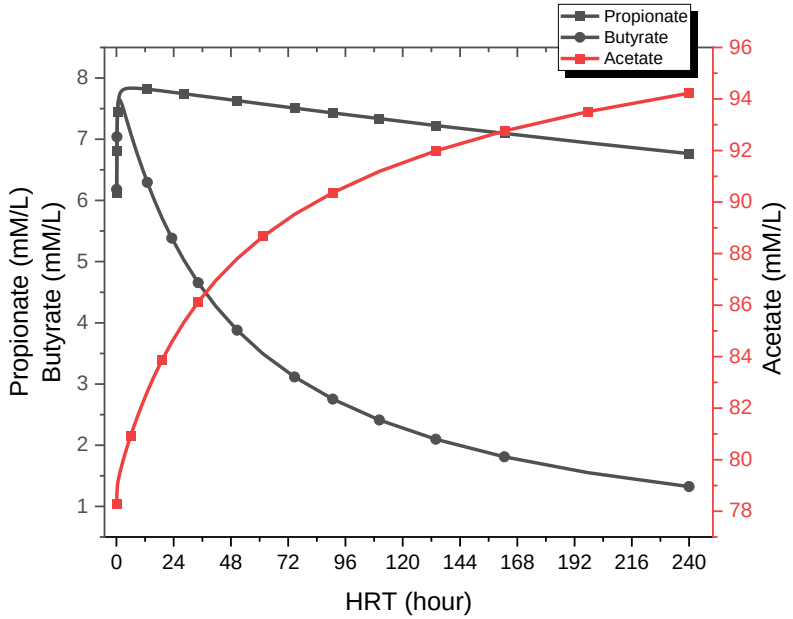

Figure 17: Accumulation of volatile fatty acids in dark fermentation process

3.2.4 Biohydrogen production in photo fermentation

Standalone simulation of biohydrogen production was investigated using the same amount of pineapple peels and organic loading rate as in dark fermentation. The main carbon sources are xylose and glucose obtained after the hydrolysis step. The kinetic data used for the simulation is derived from data provided by glucose and xylose degradation by *Rhodobacter sphaeroides*. This strain is a purple non-sulfur photosynthetic bacteria known for its ability to use efficiently a wide range of carbon sources including xylose, glucose and volatile fatty acids (Pattanamanee et al., 2015). Simulation results of cumulative biohydrogen yield as well as glucose and xylose consumption are shown on Figure 18. It can clearly be seen that the cumulative biohydrogen yield exhibits an upward trend while the concentrations of glucose and xylose decrease over time. Like in dark fermentation, the cumulative hydrogen yield spikes within the first five days and experiences more steady growth during the last five days. After running the process for 10 days of hydraulic retention time, the cumulative biohydrogen yield was 268.3 mL/g VS. From the graph it appears that during the first five days of hydraulic retention time only around 50% of initial glucose and xylose quantity were consumed. This gradual decrease in glucose and xylose concentration highlights the moderate consumption rate of both sugar by *Rhodobacter sphaeroide* strains (Pattanamanee et al., 2015).

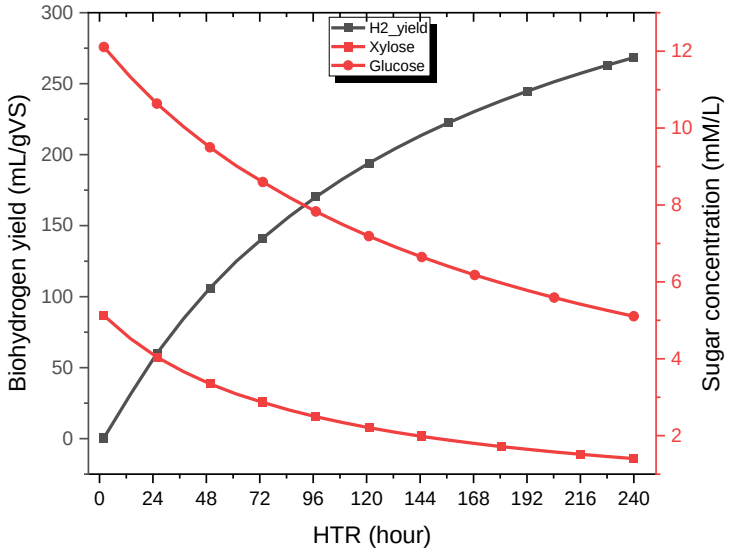

Figure 18: Cumulative hydrogen yield and substrate consumption in photo fermentation

The Table 9 presents the biohydrogen yields reported in the literature from single stage photo fermentation systems using lignocellulosic biomass as substrate. From the table, it clearly appears that the findings of the current study are slightly greater than data reported in the literature. One possible reason behind the gap observed between the current simulation result and the reported studies is the fact that the current model does not include light conversion efficiency. Light conversion efficiency is a key factor in photo fermentative hydrogen production. In fact, light conversion efficiency is a major bottleneck for scale up of biohydrogen production by photo fermentation (Jiang et al., 2022). Investigations on light conversion efficiency revealed that most photo fermentative systems seldom exceed 10 % light conversion efficiency (Jiang et al., 2022; Lu et al., 2021). More importantly when using agricultural residues as substrate, conversion rate of light energy should be taken into account as the shading ability of the substrate is high (Zhang et al., 2020).

Table 9: Biohydrogen yield from standalone photo fermentation of lignocellulosic biomass reported in literature

Type of substrate	H_2 production (mL/g TS)	Reference
Giant reed	50 - 124.3	(Shui et al., 2022)
Corn stover	141.42	(Zhang et al., 2020)
Apple waste	111.85	(Lu et al., 2016)
Corn cob	223.3 - 367.9	(Fan et al., 2022)
Corn cob	59.5 - 84.7	(Zhang et al., 2020)
Energy grasses	24.84 -147.64	(Zhang et al., 2020)
Pineapple peels	257.43	This study

3.2.5 Influence of organic loading rate on one stage photo fermentation

The Table 10 illustrates the simulation results of cumulative hydrogen yield when varying the organic loading rate from 5 to 30 gVS/L/day. Like in dark fermentation, the overall biohydrogen yield increased with the organic loading rate. Significant performances in biohydrogen were notified when the organic loading rate increased from 5 to 15 gVS/L/day. For organic loading rates above 15 gVS/L/day, the increase rate in biohydrogen yield slow down and asymptotic behavior was observed where further increases in organic loading rate result small gains in biohydrogen yield. This observation suggests an optimal organic loading rate in the range of 15 to 20 gVS/L/day. Lu et al. (2018) investigated the impact of organic loading rate on pilot scale photo fermentative system and reported an optimal organic loading rate of 20 g/L/day for maximum biohydrogen yield in continuous operation. The line graph in Figure 19 depicts the time variations of cumulative hydrogen yield at different organic loading rates. For all organic loading rates, the cumulative biohydrogen begins slow and within the first hours of fermentation with approximately the same performance in cumulative hydrogen yield (Figure 19). Following the first 24 hours of fermentation, a clear gap in cumulative biohydrogen yield performance was observed when the organic loading rate was less than 15 gVS/L/day. The saturation trend observed in Table 10 is confirmed by overlapping curves from organic loading rates above 15. In addition, from 5 to 10 days of hydraulic retention time, approximately only 10% improvement in cumulative hydrogen yield was recorded (Figure 19). Meanwhile, it will be interesting to run the system at medium organic loading rate with shorter retention time.

Table 10: Impact of organic loading rate on cumulative hydrogen yield in photo fermentation

OLR (g VS/L/day)	**H_2 yield (mL/g VS)**
5	258.63
10	268.29
15	271.52
20	273.58
25	274.25
30	274.34

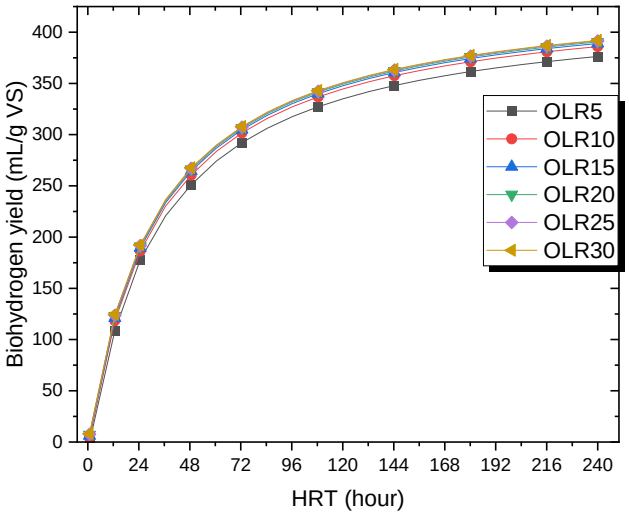

Figure 19: Impact of organic loading rate on hydrogen yield in photo fermentation

3.2.6 Hydrogen yields in sequential dark-photo fermentation

The simulation of sequential dark-photo fermentation was conducted in two stages. In the first stage, dark fermentation of pineapple peels was implemented with 4 days hydraulic retention time and 10 $gVS/L/day$. The dark fermentation residence time is short since the cumulative biohydrogen yield after 96 h is over 80 % of the overall yield after 10 days. In addition, the important quantities of volatile are produced within this short residence time will require more time in photo fermentation step. In the second stage, the effluent from dark fermentation which includes mainly volatile fatty acids (acetic, propionic and butyric acid) from dark fermentation was used as substrate to perform photo fermentation. The residence time for photo fermentation was set at 6 days to achieve a high conversion ratio of volatile fatty acids. The graph of Figure 20 shows the time course of biohydrogen and volatile fatty acids concentration. Overall, for the first four days of residence time, the graph presents similar trends previously observed in dark fermentation (subsection 3.2.1). The following days see fast consumption of volatile fatty acids and consequently high production rates of biohydrogen. The concentration of acetic acid topped at $90.61\ mM/L$ at the end of the dark fermentation stage before dropping to $20\ mM/L$ between the 6^{th} and 10^{th} day of retention time during photo fermentation stage. This result shows that approximately 78 % of acetic acid was consumed during photo fermentation. Propionic acid and butyric acid exhibit around 45 % and 68 % consumption, respectively in photo fermentation. The cumulative biohydrogen yield rose sharply from around $90\ mL/gVS$ at the end of dark fermentation and peaked at $798.67\ mL/gVS$ by the end of the 10 days of residence time.

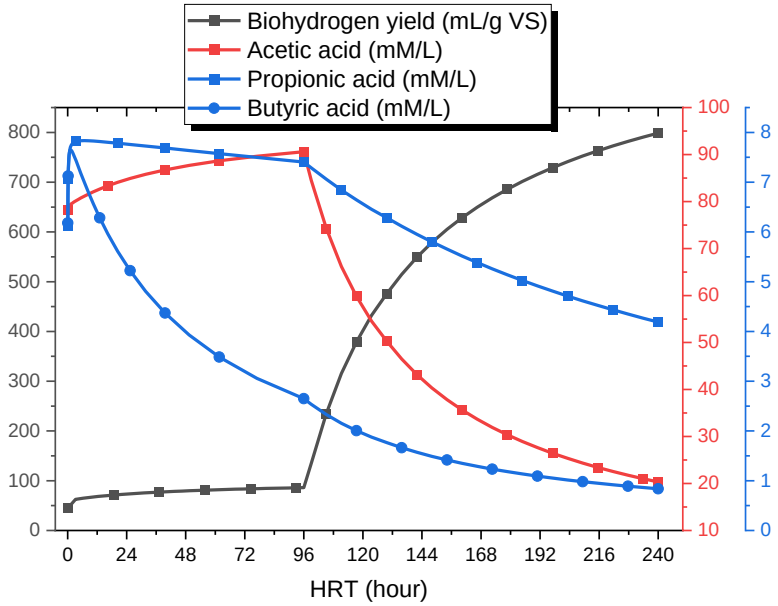

Figure 20: Cumulative hydrogen yield and volatile fatty acids consumption in sequential dark-photo fermentation

The Table 11 shows a comparison of the simulation results of the current study and reported values in the literature on two-stage dark and photo fermentation of different lignocellulosic biomasses. Overall, what stands out from the Table 11 is a significant improvement of the total cumulative biohydrogen yield through the sequential process. The current simulation results exhibit good biohydrogen production performance compared to data reported in the literature (Table 11). However, it is worth noting that hydrogen production performance in the sequential process depends on the constitution of the dark fermentation effluent and a good balance in volatile fatty acids is important to achieve good results. Acetic acid and lactic acid are good substrates for photo fermentation as they are easily metabolized by purple non sulfur bacteria (Lo et al., 2011). On the other hand, propionic acid is consumed at a lower rate, usually after acetic acid has been depleted. Its presence in high concentrations inhibits microbial cell growth and hydrogen production (Uyar et al., 2009). As far as ethanol is concerned, its presence in low concentration enhance the microbial activity of hydrogen producing bacteria, however beyond some threshold it inhibit the microbial cell growth (Jiang et al., 2025). For instance Wu et al., (2010), reported important proportion of ethanol in dark fermentation effluents and the sequential dark-photo fermentation achieved only 50 % improvement in cumulative hydrogen yield from dark fermentation stage. However, when acetic acid and butyric acid were the major components of dark fermentation effluent, a 2.4 fold enhancement was achieved by Cheng et al., (2011a) and 7.8 fold enhancement by Su et al., (2010) in their respective study. These results highlight the impact of the constitution of dark fermentation effluents on the photo fermentation process in the second stage.

Table 11: Biohydrogen yield from sequential dark- photo fermentation of lignocellulosic biomass reported in literature

Type of substrate	H_2 production		Reference
	Dark fermentation	Sequential dark-photo fermentation	
Corn stalk (mL/g)	156.7	439.4	(Zhang et al., 2017)
Bagasse (mL/g)	107.8	162.1	(Wu et al., 2010)
Water hyacinth (mL/g VS)	112.3	751.5	(Cheng et al., 2013)
Cassava starch (mL/g)	351	840	(Cheng et al., 2011a)
Corn cob (mL/g)	120.3	738.5	(Yang et al., 2010)
Water hyacinth mL/g VS	76.7	596.1	(Su et al., 2010)
Rice straw mL/g VS	155	463	(Cheng et al., 2011b)
Pineapple peels mL/g VS	86.11	798.67	This study

The heating value conversion efficiency of each process at an organic loading rate of 10 gVS/L/day is illustrated in Table 12. Dark fermentation shows the lowest heating value conversion efficiency of 6.36. This poor performance can be explained by limitations imposed by the hydrolysis step and the Thauer limit (Thauer et al., 1977) which are still important bottlenecks of the dark fermentation process. This results fell in the range of reported values in the literature when lignocellulosic biomass is used as substrate (Su et al., 2009; Zhang et al., 2020; Zhang et al., 2017). The heating value conversion efficiency for one-stage photo fermentation was 18.26 which is 1.8 fold higher than the maximum reported by Zhang, et al., (2020) in their study on photo fermentation of corn stover. The 54.36 % heating conversion efficiency recorded for the sequential process is also slightly higher than the 46% found by Su et al. (2009).

Table 12: Heating value conversion efficiency

Process	Heating value conversion efficiency (%)
Standalone dark fermentation	6.36
Standalone photo fermentation	18.26
Two-stage dark and photo fermentation	54.36

Conclusion

Conclusion

1.1 Summary

The relentless increase in sustainable energy solutions coupled with the need to sustainable valorization of agro-industrial residues creates an incentive to investigate biochemical pathways for energy conversion. In this context pineapple processing waste from JUS DELICE represents a good feedstock for bioenergy production, as its energy potential is currently unexplored.

This study assessed the potential of biohydrogen production from lignocellulosic biomass using pineapple peels as substrate collected from JUS DELICE. The pineapple peels were characterized by ultimate analysis, proximate analysis and fiber content. A baseline model was developed using Aspen Plus(v14) to predict biohydrogen production from standalone dark fermentation, standalone photo fermentation and sequential dark-photo fermentation.

Investigation into the physicochemical properties of pineapple peels revealed their favorable potential for bioenergy production through biochemical conversion. Specifically, proximate analysis indicated a high volatile solid content of 95% and a low ash content of 4 % on a dry weight basis. Furthermore, fiber analysis showed cellulose, hemicellulose and lignin content of 15.82 %, 27.79% and 3.06% respectively. Elemental analysis identified carbon (44.6 % C), oxygen (44.3 % O) and hydrogen (6.08 % H) as the dominant elements, with nitrogen (N), phosphorous (P) and sulfur (S) present in smaller quantities (0.794 %, 0.13 % and 0.1 % respectively). These properties collectively support the use of pineapple peels as an effective substrate for biohydrogen production.

Simulation results demonstrated that sequential dark-photo fermentation achieved the best performance with 798.67 mL/gVS of cumulative biohydrogen yield and 54.6% conversion efficiency based on heating value. Dark fermentation produced a cumulative hydrogen yield of 93.5 mL/gVS with 6.36% calorific value conversion efficiency. These values were in good agreement with reported values in literature. On the other hand, the cumulative hydrogen yield in photo fermentation was 268.3 mL/gVS with 18.26% conversion efficiency of heating value. These values were found to be slightly higher than those reported in the literature. Furthermore, a sensitivity analysis of the organic loading rate revealed saturation trends at values above 20 g VS/L/day in standalone dark fermentation and values above 15 g VS/L/day in one-stage photo fermentation.

1.2 Limitations

The process simulation model successfully predicted biohydrogen yield from the different conversion pathways investigated. Furthermore, the model sensitivity to organic loading rate and hydraulic retention time were successfully analyzed. Despite these successful achievements, this study has several limitations due to challenges in secondary data acquisition, time constraints and

the complexity of the implementation of biochemical processes in Aspen Plus. The main key objectives which have not been achieved are:

1) Sensitivity to initial pH;
2) Sensitivity to temperature (due to first order kinetics approximation);
3) Sensitivity to light intensity;
4) Inhibition effects of ammonia and volatile fatty acids;
5) Optimization of process parameters.

1.3 Recommendations and perspectives

As far as the valorization of pineapple peels is concerned, future research should focus on comparative study of different valorization pathways including bioethanol, composting and biomethane. The study should include techno economic assessment and life cycle analysis to identify and recommend the most viable process for pineapple waste management at JUS DELICE.

Regarding the process simulation model, several improvements to move from the baseline model to a benchmark model and make the model more realistic. This could be achieved by:

1) Implementing user defined subroutines in Fortran which use kinetic models for substrate consumption, hydrogen production and volatile fatty acids formation;
2) Include biomass dynamics (growth, decay and yield);
3) Include sensitivity to key parameters and inhibition effects via Fortran subroutines;
4) Optimize process parameters using Design Expert Software.

References

References

Aguilar, M. C., Wang, Y. D., Roskilly, T., Pathare, P. B., & Lamidi, R. O. (2017). Biogas from anaerobic co-digestion of food waste and primary sludge for cogeneration of power and heat. *Energy Procedia*, *142*, 70–76. https://doi.org/10.1016/J.EGYPRO.2017.12.012

Ahmad, A., K, R., Hasan, S. W., Show, P. L., & Banat, F. (2024). Biohydrogen production through dark fermentation: Recent trends and advances in transition to a circular bioeconomy. *International Journal of Hydrogen Energy*, *52*, 335–357. https://doi.org/10.1016/J.IJHYDENE.2023.05.161

Akbari, L., & Mahmoodzadeh Vaziri, B. (2017). Comprehensive modeling of photo-fermentation process for prediction of hydrogen production. *International Journal of Hydrogen Energy*, *42*(21), 14449–14457. https://doi.org/https://doi.org/10.1016/j.ijhydene.2017.04.119

Al-Rubaye, H., Karambelkar, S., Shivashankaraiah, M. M., & Smith, J. D. (2019). Process Simulation of Two-Stage Anaerobic Digestion for Methane Production. *Biofuels*, *10*(2), 181–191. https://doi.org/10.1080/17597269.2017.1309854

Andrews, J. F. (1968). A mathematical model for the continuous culture of microorganisms utilizing inhibitory substrates. *Biotechnology and Bioengineering*, *10*(6), 707–723. https://doi.org/10.1002/BIT.260100602

Ayaburi, J., Bazilian, M., Kincer, J., & Moss, T. (2020). Measuring "Reasonably Reliable" access to electricity services. *The Electricity Journal*, *33*(7), 106828. https://doi.org/10.1016/J.TEJ.2020.106828

Azevedo, A., Gominho, J., & Duarte, E. (2021). Performance of Anaerobic Co-digestion of Pig Slurry with Pineapple (Ananas comosus) Bio-waste Residues. *Waste and Biomass Valorization*, *12*(1), 303–311. https://doi.org/10.1007/S12649-020-00959-W/TABLES/5

Banerjee, S., Patti, A. F., Ranganathan, V., & Arora, A. (2019). Hemicellulose based biorefinery from pineapple peel waste: Xylan extraction and its conversion into xylooligosaccharides. *Food and Bioproducts Processing*, *117*, 38–50. https://doi.org/10.1016/J.FBP.2019.06.012

Banerjee, S., Ranganathan, V., Patti, A., & Arora, A. (2018). Valorisation of pineapple wastes for food and therapeutic applications. *Trends in Food Science & Technology*, *82*, 60–70. https://doi.org/10.1016/J.TIFS.2018.09.024

References

Bechara, R. (2022). Improvements to the ADM1 based Process Simulation Model: Reaction segregation, parameter estimation and process optimization. *Heliyon*, *8*(12), e11793. https://doi.org/10.1016/J.HELIYON.2022.E11793

Boshagh, F., Rostami, K., & van Niel, E. W. J. (2022). Application of kinetic models in dark fermentative hydrogen production–A critical review. *International Journal of Hydrogen Energy*, *47*(52), 21952–21968. https://doi.org/10.1016/J.IJHYDENE.2022.05.031

Carreón, N. A. D., Gurubel-Tun, K. J., Rangel, B. C. S., León-Becerril, E., & García-Depraect, O. (2022). Kinetic modelling of a dark fermentation process using tequila vinasses as substrate for hydrogen production. *Memorias Del Congreso Nacional de Control Automático*. https://doi.org/10.58571/cnca.amca.2022.040

Casabar, J. T., Unpaprom, Y., & Ramaraj, R. (2019). Fermentation of pineapple fruit peel wastes for bioethanol production. *Biomass Conversion and Biorefinery*, *9*(4), 761–765. https://doi.org/10.1007/S13399-019-00436-Y/TABLES/3

CFE. (2018). *Annonce légale JUS DELICE SA*. https://cfetogo.tg/annonces-legales/annonce-legale-annonce-legale-jus-delice-sa.html

Chen, A., Guan, Y. J., Bustamante, M., Uribe, L., Uribe-Lorío, L., Roos, M. M., & Liu, Y. (2020). Production of renewable fuel and value-added bioproducts using pineapple leaves in Costa Rica. *Biomass and Bioenergy*, *141*, 105675. https://doi.org/10.1016/J.BIOMBIOE.2020.105675

Chen, W. H., Chen, S. Y., Kumar Khanal, S., & Sung, S. (2006). Kinetic study of biological hydrogen production by anaerobic fermentation. *International Journal of Hydrogen Energy*, *31*(15), 2170–2178. https://doi.org/10.1016/J.IJHYDENE.2006.02.020

Cheng, J., Su, H., Zhou, J., Song, W., & Cen, K. (2011a). Hydrogen production by mixed bacteria through dark and photo fermentation. *International Journal of Hydrogen Energy*, *36*(1), 450–457. https://doi.org/10.1016/J.IJHYDENE.2010.10.007

Cheng, J., Su, H., Zhou, J., Song, W., & Cen, K. (2011b). Microwave-assisted alkali pretreatment of rice straw to promote enzymatic hydrolysis and hydrogen production in dark- and photo-fermentation. *International Journal of Hydrogen Energy*, *36*(3), 2093–2101.

https://doi.org/10.1016/J.IJHYDENE.2010.11.021

Cheng, J., Xia, A., Su, H., Song, W., Zhou, J., & Cen, K. (2013). Promotion of H2 production by microwave-assisted treatment of water hyacinth with dilute H2SO4 through combined dark fermentation and photofermentation. *Energy Conversion and Management*, *73*, 329–334. https://doi.org/10.1016/J.ENCONMAN.2013.05.018

Cieciura-Włoch, W., Borowski, S., & Otlewska, A. (2020). Biohydrogen production from fruit and vegetable waste, sugar beet pulp and corn silage via dark fermentation. *Renewable Energy*, *153*, 1226–1237. https://doi.org/10.1016/J.RENENE.2020.02.085

Dai, H., Huang, Y., Zhang, H., Ma, L., Huang, H., Wu, J., & Zhang, Y. (2020). Direct fabrication of hierarchically processed pineapple peel hydrogels for efficient Congo red adsorption. *Carbohydrate Polymers*, *230*, 115599. https://doi.org/10.1016/J.CARBPOL.2019.115599

Dhar, B. R., Elbeshbishy, E., & Nakhla, G. (2012). Influence of iron on sulfide inhibition in dark biohydrogen fermentation. *Bioresource Technology*, *126*, 123–130. https://doi.org/10.1016/J.BIORTECH.2012.09.043

Ding, C., Yang, K. L., & He, J. (2016). Biological and fermentative production of hydrogen. *Handbook of Biofuels Production: Processes and Technologies: Second Edition*, 303–333. https://doi.org/10.1016/B978-0-08-100455-5.00011-4

Dzulkarnain, E. L. N., Audu, J. O., Wan Dagang, W. R. Z., & Abdul-Wahab, M. F. (2022). Microbiomes of biohydrogen production from dark fermentation of industrial wastes: current trends, advanced tools and future outlook. *Bioresources and Bioprocessing 2022 9:1*, *9*(1), 1–25. https://doi.org/10.1186/S40643-022-00504-8

ECREEE, & DGE. (2024). *Togo Bioenergy Actions Plan – ECREEE*. https://www.ecreee.org/wpfd_file/togo-bioenergy-actions-plan/

Fan, X., Li, Y., Luo, Z., Jiao, Y., Ai, F., Zhang, H., Zhu, S., Zhang, Q., & Zhang, Z. (2022). Surfactant assisted microwave irradiation pretreatment of corncob: Effect on hydrogen production capacity, energy consumption and physiochemical structure. *Bioresource Technology*, *357*, 127302. https://doi.org/10.1016/J.BIORTECH.2022.127302

Foglia, D., Ljunggren, M., Wukovits, W., Friedl, A., Zacchi, G., Urbaniec, K., & Markowski, M.

(2010). Integration studies on a two-stage fermentation process for the production of biohydrogen. *Journal of Cleaner Production*, *18*(SUPPL. 1), S72–S80. https://doi.org/10.1016/J.JCLEPRO.2010.06.022

Gadhamshetty, V., Sukumaran, A., Nirmalakhandan, N., & Myint, M. T. (2008). Photofermentation of malate for biohydrogen production— A modeling approach. *International Journal of Hydrogen Energy*, *33*(9), 2138–2146. https://doi.org/10.1016/J.IJHYDENE.2008.02.046

Gafa, D. W., Egbendewe, A. Y. G., & Jodoin, L. (2022). Operationalizing affordability criterion in energy justice: Evidence from rural West Africa. *Energy Economics*, *109*, 105953. https://doi.org/https://doi.org/10.1016/j.eneco.2022.105953

Gbiete, D., Narra, S., Mani Kongnine, D., Narra, M. M., & Nelles, M. (2024). Insights into Biohydrogen Production Through Dark Fermentation of Food Waste: Substrate Properties, Inocula, and Pretreatment Strategies. *Energies 2024, Vol. 17, Page 6350*, *17*(24), 6350. https://doi.org/10.3390/EN17246350

Gharge, V., Ghutake, S., & Pawar, H. (2024). Valorization of Pineapple Waste for Extraction and Purification of Bromelain Enzyme. *ACS Sustainable Resource Management*, *1*(11), 2439–2451. https://doi.org/10.1021/ACSSUSRESMGT.4C00283

Ghimire, A., Frunzo, L., Pirozzi, F., Trably, E., Escudie, R., Lens, P. N. L., & Esposito, G. (2015). A review on dark fermentative biohydrogen production from organic biomass: Process parameters and use of by-products. *Applied Energy*, *144*, 73–95. https://doi.org/10.1016/J.APENERGY.2015.01.045

Gu, C., Kim, G. B., Kim, W. J., Kim, H. U., & Lee, S. Y. (2019). Current status and applications of genome-scale metabolic models. *Genome Biology 2019 20:1*, *20*(1), 1–18. https://doi.org/10.1186/S13059-019-1730-3

Guo, H., Oosterkamp, M. J., Tonin, F., Hendriks, A., Nair, R., van Lier, J. B., & de Kreuk, M. (2021). Reconsidering hydrolysis kinetics for anaerobic digestion of waste activated sludge applying cascade reactors with ultra-short residence times. *Water Research*, *202*, 117398. https://doi.org/10.1016/J.WATRES.2021.117398

References

Gupta, S., Fernandes, A., Lopes, A., Grasa, L., & Salafranca, J. (2024). Photo-Fermentative Bacteria Used for Hydrogen Production. *Applied Sciences 2024, Vol. 14, Page 1191*, *14*(3), 1191. https://doi.org/10.3390/APP14031191

Hallenbeck, P. C. (2009). Fermentative hydrogen production: Principles, progress, and prognosis. *International Journal of Hydrogen Energy*, *34*(17), 7379–7389. https://doi.org/https://doi.org/10.1016/j.ijhydene.2008.12.080

Hallenbeck, P. C. (2013). Fundamentals of Biohydrogen. *Biohydrogen*, 25–43. https://doi.org/10.1016/B978-0-444-59555-3.00002-7

Hallenbeck, P. C., & Ghosh, D. (2009). Advances in fermentative biohydrogen production: the way forward? *Trends in Biotechnology*, *27*(5), 287–297. https://doi.org/10.1016/J.TIBTECH.2009.02.004

Han, K., & Levenspiel, O. (1988). Extended monod kinetics for substrate, product, and cell inhibition. *Biotechnology and Bioengineering*, *32*(4), 430–447. https://doi.org/10.1002/BIT.260320404

IEA. (2022). *World - IEA*. https://www.iea.org/world/energy-mix

INSEED. (2022). *Dépliant et Communiqué RGPH – INSEED*. https://inseed.tg/depliant-et-communique-rgph/

IPCC. (2022). *The evidence is clear: the time for action is now. We can halve emissions by 2030. — IPCC*. https://www.ipcc.ch/2022/04/04/ipcc-ar6-wgiii-pressrelease/

IRENA, & AfDB. (2022). *Renewable Energy Market Analysis: Africa and its Regions*. https://www.irena.org/publications/2022/Jan/Renewable-Energy-Market-Analysis-Africa

Ji, M., & Wang, J. (2021). Review and comparison of various hydrogen production methods based on costs and life cycle impact assessment indicators. *International Journal of Hydrogen Energy*, *46*(78), 38612–38635. https://doi.org/10.1016/J.IJHYDENE.2021.09.142

Jiang, D., Zhang, L., Pei, W., Song, Z., Zhang, T., Jing, Y., Chen, Z., Li, W., Zhang, Q., & Lu, C. (2025). Correlation between ethanol addition and photo-fermentative biohydrogen production of Arundo donax L. with a consortium. *Renewable Energy*, *248*, 123077.

https://doi.org/10.1016/J.RENENE.2025.123077

Jiang, D., Zhang, X., Jing, Y., Zhang, T., Shui, X., Yang, J., Lu, C., Chen, Z., Lei, T., & Zhang, Q. (2022). Towards high light conversion efficiency from photo-fermentative hydrogen production of Arundo donax L. By light–dark duration alternation strategy. *Bioresource Technology*, *344*, 126302. https://doi.org/10.1016/J.BIORTECH.2021.126302

Kádár, Z., De Vrije, T., Van Noorden, G. E., Budde, M. A. W., Szengyel, Z., Réczey, K., & Claassen, P. A. M. (2004). Yields from glucose, xylose, and paper sludge hydrolysate during hydrogen production by the extreme thermophile Caldicellulosiruptor saccharolyticus. *Applied Biochemistry and Biotechnology - Part A Enzyme Engineering and Biotechnology*, *114*(1–3), 497–508. https://doi.org/10.1385/ABAB:114:1-3:497

Khamtib, S., & Reungsang, A. (2012). Biohydrogen production from xylose by Thermoanaerobacterium thermosaccharolyticum KKU19 isolated from hot spring sediment. *International Journal of Hydrogen Energy*, *37*(17), 12219–12228. https://doi.org/10.1016/J.IJHYDENE.2012.06.038

Kharisma, A. D., Amekan, Y., Sarto, & Cahyanto, M. N. (2022). Effect of Hydrogen Peroxide on Hydrogen Production from Melon Fruit (Cucumis melo L.) Waste by Anaerobic Digestion Microbial Community. *International Journal of Renewable Energy Development*, *11*(1), 95–101. https://doi.org/10.14710/IJRED.2022.40883

Kim, B., Jeong, J., Kim, J., Hee Yoon, H., Khanh Thinh Nguyen, P., & Kim, J. (2022). Mathematical modeling of dark fermentation of macroalgae for hydrogen and volatile fatty acids production. *Bioresource Technology*, *354*, 127193. https://doi.org/10.1016/J.BIORTECH.2022.127193

Kim, J. O., Kim, Y. H., Ryu, J. Y., Song, B. K., Kim, I. H., & Yeom, S. H. (2005). Immobilization methods for continuous hydrogen gas production biofilm formation versus granulation. *Process Biochemistry*, *40*(3–4), 1331–1337. https://doi.org/10.1016/J.PROCBIO.2004.06.008

Kombate, A., Folega, F., Atakpama, W., Dourma, M., Wala, K., & Goïta, K. (2022). Characterization of Land-Cover Changes and Forest-Cover Dynamics in Togo between 1985

and 2020 from Landsat Images Using Google Earth Engine. In *Land* (Vol. 11, Issue 11). https://doi.org/10.3390/land11111889

Kraemer, J. T., & Bagley, D. M. (2007). Improving the yield from fermentative hydrogen production. *Biotechnology Letters*, *29*(5), 685–695. https://doi.org/10.1007/s10529-006-9299-9

Lay, J. J. (2001). Biohydrogen generation by mesophilic anaerobic fermentation of microcrystalline cellulose. *Biotechnology and Bioengineering*, *74*(4), 280–287. https://doi.org/10.1002/BIT.1118

Lee, K. S., Hsu, Y. F., Lo, Y. C., Lin, P. J., Lin, C. Y., & Chang, J. S. (2008). Exploring optimal environmental factors for fermentative hydrogen production from starch using mixed anaerobic microflora. *International Journal of Hydrogen Energy*, *33*(5), 1565–1572. https://doi.org/10.1016/J.IJHYDENE.2007.10.019

Li, C., Aston, J. E., Lacey, J. A., Thompson, V. S., & Thompson, D. N. (2016). Impact of feedstock quality and variation on biochemical and thermochemical conversion. *Renewable and Sustainable Energy Reviews*, *65*, 525–536. https://doi.org/10.1016/J.RSER.2016.06.063

Liebetrau, J., Pfeiffer, D., & Thrän, D. (2016). *Collection of Methods for Biogas. Methods to determine parameters for analysis purposes and Parameters that describe processes in the biogas sector*.

Lim, S. W., & Nandong, J. (2022). Modeling of biohydrogen production using generalized multi-scale kinetic model: Impacts of fermentation conditions. *International Journal of Hydrogen Energy*, *47*(41), 17926–17945. https://doi.org/10.1016/J.IJHYDENE.2022.03.291

Lo, Y. C., Chen, C. Y., Lee, C. M., & Chang, J. S. (2011). Photo fermentative hydrogen production using dominant components (acetate, lactate, and butyrate) in dark fermentation effluents. *International Journal of Hydrogen Energy*, *36*(21), 14059–14068. https://doi.org/10.1016/J.IJHYDENE.2011.04.148

Lo, Y. C., Chen, W. M., Hung, C. H., Chen, S. Der, & Chang, J. S. (2008). Dark H2 fermentation from sucrose and xylose using H2-producing indigenous bacteria: Feasibility and kinetic studies. *Water Research*, *42*(4–5), 827–842. https://doi.org/10.1016/J.WATRES.2007.08.023

References

Logan, B. E., Oh, S. E., Kim, I. S., & Van Ginkel, S. (2002). Biological hydrogen production measured in batch anaerobic respirometers. *Environmental Science and Technology*, *36*(11), 2530–2535. https://doi.org/10.1021/ES015783I/ASSET/IMAGES/MEDIUM/ES015783IE00002.GIF

Lorenzo-Llanes, J., Pagés-Díaz, J., Kalogirou, E., & Contino, F. (2020). Development and application in Aspen Plus of a process simulation model for the anaerobic digestion of vinasses in UASB reactors: Hydrodynamics and biochemical reactions. *Journal of Environmental Chemical Engineering*, *8*(2), 103540. https://doi.org/10.1016/J.JECE.2019.103540

Lu, C., Li, W., Zhang, Q., Liu, L., Zhang, N., Qu, B., Yang, X., Xu, R., Chen, J., & Sun, Y. (2021). Enhancing photo-fermentation biohydrogen production by strengthening the beneficial metabolic products with catalysts. *Journal of Cleaner Production*, *317*. https://doi.org/10.1016/j.jclepro.2021.128437

Lu, C., Zhang, Z., Ge, X., Wang, Y., Zhou, X., You, X., Liu, H., & Zhang, Q. (2016). Bio-hydrogen production from apple waste by photosynthetic bacteria HAU-M1. *International Journal of Hydrogen Energy*, *41*(31), 13399–13407. https://doi.org/10.1016/J.IJHYDENE.2016.06.101

Lu, C., Zhang, Z., Zhou, X., Hu, J., Ge, X., Xia, C., Zhao, J., Wang, Y., Jing, Y., Li, Y., & Zhang, Q. (2018). Effect of substrate concentration on hydrogen production by photo-fermentation in the pilot-scale baffled bioreactor. *Bioresource Technology*, *247*, 1173–1176. https://doi.org/10.1016/J.BIORTECH.2017.07.122

Madureira, A. R., Atatoprak, T., Çabuk, D., Sousa, F., Pullar, R. C., & Pintado, M. (2018). Extraction and characterisation of cellulose nanocrystals from pineapple peel. *International Journal of Food Studies*, *7*(1), 24–33. https://doi.org/10.7455/IJFS/7.1.2018.A3

Magama, P., Chiyanzu, I., & Mulopo, J. (2021). *Investigating Dark Fermentation as a Sustainable Organic Waste Management Technology for Producing Biohydrogen From Fruit and Vegetable Waste*. https://doi.org/10.21203/RS.3.RS-955255/V1

Mala, T., Piayura, S., & Itthivadhanapong, P. (2024). Characterization of dried pineapple (Ananas comosus L.) peel powder and its application as a novel functional food ingredient in cracker

product. *Future Foods*, *9*, 100322. https://doi.org/10.1016/J.FUFO.2024.100322

Marcondes dos Santos, H. T., & Perrella Balestieri, J. A. (2018). Spatial analysis of sustainable development goals: A correlation between socioeconomic variables and electricity use. *Renewable and Sustainable Energy Reviews*, *97*, 367–376. https://doi.org/https://doi.org/10.1016/j.rser.2018.08.037

McDowall, J. S., Murphy, B. J., Haumann, M., Palmer, T., Armstrong, F. A., & Sargent, F. (2014). Bacterial formate hydrogenlyase complex. *Proceedings of the National Academy of Sciences of the United States of America*, *111*(38), E3948–E3956. https://doi.org/10.1073/PNAS.1407927111/SUPPL_FILE/PNAS.201407927SI.PDF

Mechery, J., Kumar, C. S. P., Ambily, V., Varghese, A., & Sylas, V. P. (2024). Dark fermentation of pretreated hydrolysates of pineapple fruit waste for the production of biohydrogen using bacteria isolated from wastewater sources. *Environmental Technology (United Kingdom)*, *45*(10), 2067–2075. https://doi.org/10.1080/09593330.2022.2164743;SUBPAGE:STRING:ACCESS

Meena, L., Sengar, A. S., Neog, R., & Sunil, C. K. (2022). Pineapple processing waste (PPW): bioactive compounds, their extraction, and utilisation: a review. *Journal of Food Science and Technology*, *59*(11), 4152–4164. https://doi.org/10.1007/s13197-021-05271-6

Melitos, G., Voulkopoulos, X., & Zabaniotou, A. (2021). Waste to Sustainable Biohydrogen Production Via Photo-Fermentation and Biophotolysis − A Systematic Review. *Renewable Energy and Environmental Sustainability*, *6*, 45. https://doi.org/10.1051/REES/2021047

Ministère de l'agriculture. (2020). *Filière ananas, une culture en pleine extension au Togo - Ministère de l''agriculture, de l'Hydraulique Villageoise et du Développement Rural*. https://agriculture.gouv.tg/filiere-ananas-une-culture-en-pleine-extension-au-togo/

Ministère de l'agriculture. (2023). *PLAN D'ACTION D'INVESTISSEMENT DE LA FILIERE ANANAS 2024 - 2028*.

Mizuno, O., Ohara, T., Shinya, M., & Noike, T. (2000). Characteristics of hydrogen production from bean curd manufacturing waste by anaerobic microflora. *Water Science and Technology*, *42*(3–4), 345–350. https://doi.org/10.2166/WST.2000.0401

References

Mokhtarani, B., Zanganeh, J., & Moghtaderi, B. (2025). A Review on Biohydrogen Production Through Dark Fermentation, Process Parameters and Simulation. In *Energies* (Vol. 18, Issue 5). https://doi.org/10.3390/en18051092

Monod, J. (1949). THE GROWTH OF BACTERIAL CULTURES. *Annual Review of Microbiology*, *3*(Volume 3, 1949), 371–394. https://doi.org/10.1146/ANNUREV.MI.03.100149.002103

Mu, Y., Wang, G., & Yu, H. Q. (2006). Kinetic modeling of batch hydrogen production process by mixed anaerobic cultures. *Bioresource Technology*, *97*(11), 1302–1307. https://doi.org/10.1016/J.BIORTECH.2005.05.014

Mu, Y., Zheng, X. J., Yu, H. Q., & Zhu, R. F. (2006). Biological hydrogen production by anaerobic sludge at various temperatures. *International Journal of Hydrogen Energy*, *31*(6), 780–785. https://doi.org/10.1016/J.IJHYDENE.2005.06.016

Namsree, P., Suvajittanont, W., Puttanlek, C., Uttapap, D., & Rungsardthong, V. (2012). Anaerobic digestion of pineapple pulp and peel in a plug-flow reactor. *Journal of Environmental Management*, *110*, 40–47. https://doi.org/10.1016/J.JENVMAN.2012.05.017

Nath, P. C., Ojha, A., Debnath, S., Neetu, K., Bardhan, S., Mitra, P., Sharma, M., Sridhar, K., & Nayak, P. K. (2023). Recent advances in valorization of pineapple (Ananas comosus) processing waste and by-products: A step towards circular bioeconomy. *Trends in Food Science & Technology*, *136*, 100–111. https://doi.org/10.1016/J.TIFS.2023.04.008

NDC Partnership. (2021). *Togo | NDC Partnership*. https://ndcpartnership.org/country/tgo

Nosrati-Ghods, N., Naidoo, M., Harrison, S. T. L., Isafiade, A. J., & Tai, S. L. (2020). Embedding Aspen Custom Modeller for Bioethanol Fermentation Into the Aspen Plus Flowsheet Simulator. *Chemical Engineering Transactions*, *80*, 289–294. https://doi.org/10.3303/CET2080049

Osman, A. I., Deka, T. J., Baruah, D. C., & Rooney, D. W. (2023). Critical challenges in biohydrogen production processes from the organic feedstocks. *Biomass Conversion and Biorefinery*, *13*(10), 8383–8401. https://doi.org/10.1007/s13399-020-00965-x

Paepatung, N., & Nopharatana, A. (2009). *Bio-Methane Potential of Biological Solid Materials*

and Agricultural Wastes.

Parra, R., Chicaiza-Ortiz, C., Herrera-Feijoo, R. J., Arellano-Yasaca, D. V., Lee, L.-C., Supe-Tulcan, R. X., & Marti-Herrero, J. (2025). Advancements of Biohydrogen Production Based on Anaerobic Digestion: Technologies, Substrates, and Future Prospects. *Sci 2025, Vol. 7, Page 52*, *7*(2), 52. https://doi.org/10.3390/SCI7020052

Pattanamanee, W., Chisti, Y., & Choorit, W. (2015). Photofermentive hydrogen production by Rhodobacter sphaeroides S10 using mixed organic carbon: Effects of the mixture composition. *Applied Energy*, *157*, 245–254. https://doi.org/10.1016/J.APENERGY.2015.08.027

Paz-Arteaga, S. L., Cadena-Chamorro, E., Goméz-García, R., Serna-Cock, L., Aguilar, C. N., Torres-León, C., & Co, E. C. (2024). *Unraveling the Valorization Potential of Pineapple Waste to Obtain Value-Added Products towards a Sustainable Circular Bioeconomy*. https://doi.org/10.3390/su16167236

Pérez-Rangel, M., Barboza-Corona, J. E., & Valdez-Vazquez, I. (2023). Effect of the organic loading rate and temperature on hydrogen production via consolidated bioprocessing of raw lignocellulosic substrate. *International Journal of Hydrogen Energy*, *48*(92), 35907–35918. https://doi.org/10.1016/J.IJHYDENE.2023.05.329

Rajendran, K., Kankanala, H. R., Lundin, M., & Taherzadeh, M. J. (2014). A novel process simulation model (PSM) for anaerobic digestion using Aspen Plus. *Bioresource Technology*, *168*, 7–13. https://doi.org/10.1016/J.BIORTECH.2014.01.051

Ravendran, R. R., Abdulrazik, A., & Zailan, R. (2019). Aspen Plus simulation of optimal biogas production in anaerobic digestion process. *IOP Conference Series: Materials Science and Engineering*, *702*(1), 012001. https://doi.org/10.1088/1757-899X/702/1/012001

Ren, N., Cao, G., Wang, A., Lee, D. J., Guo, W., & Zhu, Y. (2008). Dark fermentation of xylose and glucose mix using isolated Thermoanaerobacterium ihermosaccharolyticum W16. *International Journal of Hydrogen Energy*, *33*(21), 6124–6132. https://doi.org/10.1016/J.IJHYDENE.2008.07.107

Ruzicka, M. (1996). An extension of the Mosey model. *Water Research*, *30*(10), 2440–2446.

https://doi.org/10.1016/0043-1354(96)00111-X

Sağır, E., Yucel, M., & Hallenbeck, P. C. (2018). Demonstration and optimization of sequential microaerobic dark- and photo-fermentation biohydrogen production by immobilized Rhodobacter capsulatus JP91. *Bioresource Technology*, *250*, 43–52. https://doi.org/10.1016/j.biortech.2017.11.018

Sasikala, K., Ramana, C. V., & Raghuveer Rao, P. (1991). Environmental regulation for optimal biomass yield and photoproduction of hydrogen by Rhodobacter sphaeroides O.U. 001. *International Journal of Hydrogen Energy*, *16*(9), 597–601. https://doi.org/10.1016/0360-3199(91)90082-T

Schattauer, A., Abdoun, E., Weiland, P., Plöchl, M., & Heiermann, M. (2011). Abundance of trace elements in demonstration biogas plants. *Biosystems Engineering*, *108*(1), 57–65. https://doi.org/10.1016/J.BIOSYSTEMSENG.2010.10.010

Schuchmann, K., & Müller, V. (2012). A bacterial electron-bifurcating hydrogenase. *Journal of Biological Chemistry*, *287*(37), 31165–31171. https://doi.org/10.1074/jbc.M112.395038

Shui, X., Jiang, D., Zhang, H., Zhang, X., Yang, J., Lei, T., Chen, Z., & Zhang, Q. (2022). Effect of light perturbation on the photo-fermentative hydrogen production of biomass from giant reed. *Journal of Cleaner Production*, *351*, 131481. https://doi.org/10.1016/J.JCLEPRO.2022.131481

SIE. (2022). *Système d'Information Energétique du Togo*. https://eis.ecowas.int/assets/front/medias/doc/media_20240515120415.pdf

Sparling, R., Risbey, D., & Poggi-Varaldo, H. M. (1997). Hydrogen production from inhibited anaerobic composters. *International Journal of Hydrogen Energy*, *22*(6), 563–566. https://doi.org/10.1016/S0360-3199(96)00137-1

Su, H., Cheng, J., Zhou, J., Song, W., & Cen, K. (2009). Combination of dark- and photo-fermentation to enhance hydrogen production and energy conversion efficiency. *International Journal of Hydrogen Energy*, *34*(21), 8846–8853. https://doi.org/10.1016/J.IJHYDENE.2009.09.001

Su, H., Cheng, J., Zhou, J., Song, W., & Cen, K. (2010). Hydrogen production from water hyacinth

through dark- and photo- fermentation. *International Journal of Hydrogen Energy*, *35*(17), 8929–8937. https://doi.org/10.1016/J.IJHYDENE.2010.06.035

Tamiya, H., Hase, E., Shibata, K., Mituya, A., Iwamura, T., Nihei, T., & Sasa, T. (1953). Kinetics of growth of Chlorella, with special reference to its dependence on quantity of available light and on temperature. *Algal Culture from Laboratory to Pilot Plant*, 204–232.

Tawfik, A., & Salem, A. (2012). The effect of organic loading rate on bio-hydrogen production from pre-treated rice straw waste via mesophilic up-flow anaerobic reactor. *Bioresource Technology*, *107*, 186–190. https://doi.org/10.1016/J.BIORTECH.2011.11.086

Thauer, R. K., Jungermann, K., & Decker, K. (1977). Energy conservation in chemotrophic anaerobic bacteria. *Bacteriological Reviews*, *41*(1), 100–180. https://doi.org/10.1128/br.41.1.100-180.1977

Tiang, M. F., Fitri Hanipa, M. A., Abdul, P. M., Jahim, J. M. d., Mahmod, S. S., Takriff, M. S., Lay, C. H., Reungsang, A., & Wu, S. Y. (2020). Recent advanced biotechnological strategies to enhance photo-fermentative biohydrogen production by purple non-sulphur bacteria: An overview. *International Journal of Hydrogen Energy*, *45*(24), 13211–13230. https://doi.org/10.1016/J.IJHYDENE.2020.03.033

Tiegam Tagne, R. F., Costa, P., Casella, S., & Favaro, L. (2024). Optimization of biohydrogen production by dark fermentation of African food-processing waste streams. *International Journal of Hydrogen Energy*, *49*, 266–276. https://doi.org/10.1016/J.IJHYDENE.2023.07.348

Tiegam Tagne, R. F., Costa, P., Gupte, A. P., Corte, L., Casella, S., & Favaro, L. (2024). Efficient production of biohydrogen from African lignocellulosic residues. *Sustainable Energy Technologies and Assessments*, *72*, 104060. https://doi.org/10.1016/J.SETA.2024.104060

TOGO FIRST. (2022). *Togo : plus de 44.000 tonnes d'ananas produites en 2022 - Togo First*. https://www.togofirst.com/fr/agro/1811-10963-togo-plus-de-44-000-tonnes-d-ananas-produites-en-2022

Uyar, B., Eroglu, I., Yücel, M., & Gündüz, U. (2009). Photofermentative hydrogen production from volatile fatty acids present in dark fermentation effluents. *International Journal of*

Hydrogen Energy, *34*(10), 4517–4523. https://doi.org/10.1016/J.IJHYDENE.2008.07.057

Vardar-Schara, G., Maeda, T., & Wood, T. K. (2008). Metabolically engineered bacteria for producing hydrogen via fermentation. *Microbial Biotechnology*, *1*(2), 107–125. https://doi.org/10.1111/J.1751-7915.2007.00009.X

Ventura, R. L. G., Ventura, J. R. S., & Oh, Y. S. (2016). Investigation of the Photoheterotrophic Hydrogen Production of Rhodobacter sphaeroides KCTC 1434 using Volatile Fatty Acids under Argon and Nitrogen Headspace. *American Journal of Environmental Sciences*, *12*(6), 358–369. https://doi.org/10.3844/AJESSP.2016.358.369

Wang, C. C., Chang, C. W., Chu, C. P., Lee, D. J., Chang, B. V., Liao, C. S., & Tay, J. H. (2003). Using filtrate of waste biosolids to effectively produce bio-hydrogen by anaerobic fermentation. *Water Research*, *37*(11), 2789–2793. https://doi.org/10.1016/S0043-1354(03)00004-6

Wang, J., & Wan, W. (2009a). Factors influencing fermentative hydrogen production: A review. *International Journal of Hydrogen Energy*, *34*(2), 799–811. https://doi.org/10.1016/J.IJHYDENE.2008.11.015

Wang, J., & Wan, W. (2009b). Kinetic models for fermentative hydrogen production: A review. *International Journal of Hydrogen Energy*, *34*(8), 3313–3323. https://doi.org/10.1016/J.IJHYDENE.2009.02.031

Wang, W., Liu, S., & Li, Y. (2023). Modeling of biohydrogen production by dark fermentation. *Waste to Renewable Biohydrogen: Numerical Modelling and Sustainability Assessment: Volume 2*, 1–14. https://doi.org/10.1016/B978-0-12-821675-0.00009-8

WHO. (2023). *Basic energy access lags amid renewable opportunities, new report shows*. https://www.who.int/news/item/06-06-2023-basic-energy-access-lags-amid-renewable-opportunities--new-report-shows

Wu, X., Li, Q., Dieudonne, M., Cong, Y., Zhou, J., & Long, M. (2010). Enhanced H2 gas production from bagasse using adhE inactivated Klebsiella oxytoca HP1 by sequential dark-photo fermentations. *Bioresource Technology*, *101*(24), 9605–9611. https://doi.org/10.1016/J.BIORTECH.2010.07.095

References

Yaashikaa, P. R., Senthil Kumar, P., & Varjani, S. (2022). Valorization of agro-industrial wastes for biorefinery process and circular bioeconomy: A critical review. *Bioresource Technology*, *343*, 126126. https://doi.org/10.1016/J.BIORTECH.2021.126126

Yang, H., Guo, L., & Liu, F. (2010). Enhanced bio-hydrogen production from corncob by a two-step process: Dark- and photo-fermentation. *Bioresource Technology*, *101*(6), 2049–2052. https://doi.org/10.1016/J.BIORTECH.2009.10.078

Yang, H., Shi, B., Ma, H., & Guo, L. (2015). Enhanced hydrogen production from cornstalk by dark- and photo-fermentation with diluted alkali-cellulase two-step hydrolysis. *International Journal of Hydrogen Energy*, *40*(36), 12193–12200. https://doi.org/10.1016/J.IJHYDENE.2015.07.062

Yao, F., Guanghao, L., Hongyuan, M., & Lusi, Z. (2013). The Effect of Magnesium Ions on the Hydrogen-Producing Bacteria in the Water during the Ecological Restoration Process. *Advanced Materials Research*, *610–613*, 264–267. https://doi.org/10.4028/WWW.SCIENTIFIC.NET/AMR.610-613.264

Zagrodnik, R., & Duber, A. (2024). Continuous dark-photo fermentative H2 production from synthetic lignocellulose hydrolysate with different photoheterotrophic cultures: Sequential vs. co-culture processes. *Energy*, *290*, 130105. https://doi.org/10.1016/J.ENERGY.2023.130105

Zainal, B. S., Ker, P. J., Mohamed, H., Ong, H. C., Fattah, I. M. R., Rahman, S. M. A., Nghiem, L. D., & Mahlia, T. M. I. (2024). Recent advancement and assessment of green hydrogen production technologies. *Renewable and Sustainable Energy Reviews*, *189*, 113941. https://doi.org/10.1016/J.RSER.2023.113941

Zhang, T., Jiang, D., Zhang, H., Jing, Y., Tahir, N., Zhang, Y., & Zhang, Q. (2020). Comparative study on bio-hydrogen production from corn stover: Photo-fermentation, dark-fermentation and dark-photo co-fermentation. *International Journal of Hydrogen Energy*, *45*(6), 3807–3814. https://doi.org/https://doi.org/10.1016/j.ijhydene.2019.04.170

Zhang, T., Jiang, D., Zhang, H., Lee, D. J., Zhang, Z., Zhang, Q., Jing, Y., Zhang, Y., & Xia, C. (2020). Effects of different pretreatment methods on the structural characteristics, enzymatic

saccharification and photo-fermentative bio-hydrogen production performance of corn straw. *Bioresource Technology*, *304*, 122999. https://doi.org/10.1016/J.BIORTECH.2020.122999

Zhang, X. W., Zhang, Y. M., & Chen, F. (1998). Kinetic models for phycocyanin production by high cell density mixotrophic culture of the microalga Spirulina platensis. *Journal of Industrial Microbiology and Biotechnology*, *21*(6), 283–288.

Zhang, Y., Li, Q., Wang, X., Yang, H., & Guo, L. (2017). Enhanced biohydrogen production from cornstalk through a two-step fermentation: Dark fermentation and photofermentation. *International Journal of Energy Research*, *41*(15), 2491–2501. https://doi.org/10.1002/ER.3810

Zhang, Y., Zhang, H., Lee, D. J., Zhang, T., Jiang, D., Zhang, Z., & Zhang, Q. (2020). Effect of enzymolysis time on biohydrogen production from photo-fermentation by using various energy grasses as substrates. *Bioresource Technology*, *305*, 123062. https://doi.org/10.1016/J.BIORTECH.2020.123062

Zhang, Z., Li, Y., Zhang, H., He, C., & Zhang, Q. (2017). Potential use and the energy conversion efficiency analysis of fermentation effluents from photo and dark fermentative bio-hydrogen production. *Bioresource Technology*, *245*, 884–889. https://doi.org/10.1016/J.BIORTECH.2017.09.037

Zhang, Z., Zhang, H., Li, Y., Lu, C., Zhu, S., He, C., Ai, F., & Zhang, Q. (2020). Investigation of the interaction between lighting and mixing applied during the photo-fermentation biohydrogen production process from agricultural waste. *Bioresource Technology*, *312*, 123570. https://doi.org/10.1016/J.BIORTECH.2020.123570

Zwietering, M. H., Jongenburger, I., Rombouts, F. M., & Van't Riet, K. (1990). Modeling of the Bacterial Growth Curve. *Applied and Environmental Microbiology*, *56*(6), 1875. https://doi.org/10.1128/AEM.56.6.1875-1881.1990